Eur. Phys. J. C 2, 503–528 (1998)
DOI 10.1007/s100529800705

THE EUROPEAN PHYSICAL JOURNAL C

Bileptons: present limits and future prospects

Frank Cuypers[1], Sacha Davidson[2]

[1] Paul Scherrer Institute, CH-5232 Villigen PSI, Switzerland (e-mail: cuypers@pss058.psi.ch)
[2] Max-Planck-Institut für Physik, Föhringer Ring 6, D-80805 München, Germany (e-mail: sacha@mppmu.mpg.de)

Received: 24 April 1997 / Published online: 20 February 1998

Abstract. We define bileptons to be bosons coupling to a pair of leptons and construct the most general dimension four lagrangian involving scalar and vector bileptons. We concentrate on fields with lepton number 2, and derive model independent bounds on their masses and couplings from low-energy data. In addition, we study their signals in high-energy experiments and forecast the discovery potential of future colliders.

1 Introduction

The standard model of strong and electroweak interactions describes present data very successfully. However, it is commonly believed that it is not the end of the story: grand unified theories appeal to our craving for elegance, and naturalness arguments lead many theorists to believe that there should be some new physics lurking at the TeV scale. However, opinions differ on how to extend the standard model.

One of the peculiar features of the standard model is that none of its bosons carry global quantum numbers; only the fermions carry baryon or lepton number. This is no longer the case in most popular extensions. For instance, the scalar spartners in the supersymmetric standard model carry the same baryon or lepton number as their associated fermions. Grand unified theories, technicolour, and compositeness scenarios often predict the existence of light leptoquarks, di- or bileptons, and diquarks. These scalar or vector bosons respectively have baryon and/or lepton number conserving couplings to a lepton and a quark, two leptons, or two quarks.

We define a bilepton to be a boson which couples minimally (*i.e.*, with dimension four interactions) to two standard model leptons (we do not include right-handed neutrinos), but not to quarks. These particles can carry lepton number $L = 0$ or 2. They have previously shared the name "dilepton" with events having two final state leptons; to reduce confusion, we call these particles "bileptons", following Frampton [1]. We shall concentrate here on the $L = 2$ bileptons (*i.e.*, those which carry two units of lepton number L), since the $L = 0$ bileptons have very similar properties to the familiar standard model bosons.

Our aim is to provide a general and exhaustive classification of bileptons, along the same lines as the leptoquark classification performed ten years ago by Buchmüller, Rückl and Wyler [2]. Moreover, similarly to what has been done previously for leptoquarks [3], we intend to list the present bounds on bileptons that can be calculated from low-energy physics and from LEP, and to explore bounds on bileptons from future high-energy experiments. We mainly deal with discovery limits and will not dwell on the issue of uniquely determining the quantum numbers of the bileptons.

Bileptons are present in many extensions of the standard model. Scalars appear in models that generate neutrino majorana masses (see, for instance, [4–7]), and in various theories with enlarged Higgs sectors (such as left-right models [8–10]). Massive gauge bileptons may appear when the standard model is embedded in a larger gauge group [11–14], and non-gauge vectors can appear in composite and technicolour theories [15].

Various authors have previously studied constraints on bileptons. The low-energy bounds were computed in a model independent way in [16–18]. Constraints and possible collider signals for specific models have been calculated in [19–43]. More recently, the bounds on new physics following from the improved τ data have been calculated [44]. In this paper, we catalogue the low- and high-energy constraints in as complete and model independent a way as possible. We also present the bounds assuming three representative models for the generation structure of the bilepton-fermion-fermion coupling.

This work is divided into three parts. First, we write down a rather general class of bilepton lagrangians, which encompasses our definition of *bosons which couple minimally to leptons but not to quarks*. We then derive the present low-energy bounds on the bilepton couplings and masses. Finally, we compute the limits set by LEP1 and predict the bilepton coupling and mass ranges which future high-energy experiments can cover.

2 Lagrangians

In this section, we construct the most general lepton number conserving renormalisable lagrangian, consistent with electroweak symmetry, that involves standard model gauge bosons, leptons and the scalar or vector bileptons. The bilepton-lepton-lepton couplings, which we do not require to conserve lepton flavour, are free parameters. They may be very small, in which case bileptons would have little effect on low-energy data. However, the lowest dimensional couplings to the photon and Z^0 are always finite and sizable, so bileptons within the kinematically allowed mass range can always be produced at colliders.

2.1 Interactions with leptons

We consider the most general $SU(2)_L \otimes U(1)_Y$ invariant dimension four lagrangian coupling bosons to two leptons. We require the interactions to conserve lepton number, but not lepton family number. We separate the lagrangian into a part involving $L = 0$ bileptons, and a part involving $L = 2$ bileptons:

$$\begin{aligned}\mathcal{L}_{L=0} = {} & g_1 \bar{\ell}\gamma_\mu \ell L_1^\mu + \tilde{g}_1 \bar{e}\gamma_\mu e \tilde{L}_1^\mu \\ & + \tilde{g}_2 \bar{\ell} e L_2 + \text{ h.c.} \\ & + g_3 \bar{\ell}\gamma_\mu \sigma \ell \cdot \mathbf{L_3^\mu}\end{aligned} \tag{1}$$

$$\begin{aligned}\mathcal{L}_{L=2} = {} & \lambda_1 \bar{\ell}^c i\sigma_2 \ell L_1 + \text{ h.c.} + \tilde{\lambda}_1 \bar{e}^c e \tilde{L}_1 + \text{ h.c.} \\ & + \lambda_2 \bar{\ell}^c \gamma_\mu e L_2^\mu + \text{ h.c.} \\ & + \lambda_3 \bar{\ell}^c i\sigma_2 \sigma \ell \cdot \mathbf{L_3} + \text{ h.c. .}\end{aligned} \tag{2}$$

We have used the notation where $\ell = (e_L, \nu_L)$ are left-handed $SU(2)_L$ lepton doublets and $e = e_R$ are right-handed charged singlet leptons. The flavour indices are suppressed. The charge conjugate fields in $\mathcal{L}_{L=2}$ are defined to be $\bar{\ell}^c = (\ell^c)^\dagger \gamma^o = -\ell^T C^{-1}$. The subscript of the bilepton fields $L_{1,2,3}$ indicates their $SU(2)_L$ singlet, doublet or triplet nature, and the σs are the Pauli matrices. The vector bileptons also carry the Lorentz index μ. We list the quantum numbers of the bileptons in Table 2.1.

In principle derivative couplings could also be considered. However, these higher dimensional operators would be suppressed below the bilepton mass scale. We therefore concentrate on the minimal lagrangians (1, 2).

The $L = 0$ bileptons are familiar fields, as they resemble the electroweak gauge vectors and the neutral and charged Higgs scalars. Particles of this type have been of great interest in particle phenomenology during the past decades, and many publications have already been devoted to this topic. In addition, there is no compelling reason to prevent these fields from also coupling to quarks[1], so we do not consider the $L = 0$ bileptons any further here.

We rewrite the lagrangian for the $L = 2$ bileptons (2), which are the ones we wish to study, with explicit electron e and neutrino ν fields, their flavour indices ($i, j = 1, 2, 3$) and the helicity projectors $P_{R/L} = 1/2(1 \pm \gamma_5)$. The bilepton superscript is its electric charge:

$$\begin{aligned}\mathcal{L}_{L=2} = {} & -\lambda_1^{ij} \quad L_1^+ \quad \left(\bar{e}_i^c P_L \nu_j - \bar{e}_j^c P_L \nu_i\right) \\ & +\tilde{\lambda}_1^{ij} \quad \tilde{L}_1^{++} \quad \bar{e}_i^c P_R e_j \\ & +\lambda_2^{ij} \quad L_{2\mu}^+ \quad \bar{\nu}_i^c \gamma^\mu P_R e_j \\ & +\lambda_2^{ij} \quad L_{2\mu}^{++} \quad \bar{e}_i^c \gamma^\mu P_R e_j \\ & +\sqrt{2}\lambda_3^{ij} \quad L_3^0 \quad \bar{\nu}_i^c P_L \nu_j \\ & -\lambda_3^{ij} \quad L_3^+ \quad \left(\bar{e}_i^c P_L \nu_j + \bar{e}_j^c P_L \nu_i\right) \\ & -\sqrt{2}\lambda_3^{ij} \quad L_3^{++} \quad \bar{e}_i^c P_L e_j \\ & + \text{h.c. .}\end{aligned} \tag{3}$$

If the scalar L_3 acquires a vacuum expectation value it becomes the familiar $L = 2$ triplet that appears in left-right symmetric models and in the Gelmini-Roncadelli majoron model. In this case, L_3^{--} is then the well-studied doubly-charged Higgs [45] and couples to a pair of like-sign W bosons via the lepton number violating vacuum expectation value. These doubly-charged Higgs bosons can be singly produced via W fusion in hadron collisions [46]. Unfortunately, the production rates at LHC are so low that only masses up to 1.2 TeV can be probed [47]. In any case, the triplet vacuum expectation value is generically required to be small because of the smallness of $\rho - 1$, so we will assume here that it is zero.

2.2 Leptonic couplings matrices

It is clear from the lagrangian (3) that the coupling matrix for L_1 is antisymmetric in flavour space, whereas $\tilde{L}_1$ and L_3 have flavour symmetric couplings. The isosinglet L_1 corresponds to the antisymmetric part of the cross product of two doublets, and the triplet L_3 to the symmetric part. In contrast, the vector L_2 can have an arbitrary 3×3 coupling matrix. For simplicity, we will assume that all the coupling constant matrices are real. This means we are neglecting CP violation, and our bounds are really constraints on $|\lambda|$ rather than λ. Constraints from CP violation were included in the analysis of [16–18].

The aim of this paper is to discuss bileptons in a model independent way. We will list the low-energy constraints that we derive in Sect. 2 without making assumptions about the structure of the coupling matrices λ (except in the case of $\mu \to e\gamma$, see Sect. 3.1.4). However, most of the low-energy constraints arise from the non-observation of flavour violation induced by off-diagonal matrix elements. This makes the model-independent bounds difficult to interpret (see Tables 3 and 4 in Sect. 3.4). We will therefore also list the low-energy bounds using three representative models of coupling matrices, which we briefly review now.

[1] Three of the four $L = 2$ multiplets contain a doubly-charged element, which can not couple to ordinary quarks. Furthermore, if the $L = 2$ bileptons also interact with quarks of the first generation, they could mediate fast proton decay

Table 1. Major quantum numbers and couplings of the bileptons

	L	J	Y	T_3	Q_γ	Q_Z	lepton couplings	familiar sibling
L_1^μ	0	1	0	0	0	0	$\bar{e}_L e_L$ (g_1) $\bar{\nu}_L \nu_L$ (g_1)	γ Z^0 Z'
$\tilde{L}_1^\mu$	0	1	0	0	0	0	$\bar{e}_R e_R$ $(\tilde{g}_1)$	γ Z^0 Z'
L_2	0	0	1/2	1/2	1	$-\frac{2\sin^2\theta_w - 1}{2\sin\theta_w\cos\theta_w}$	$\bar{\nu}_L e_R$ (g_2)	H^+
				$-1/2$	0	$-\frac{1}{2\sin\theta_w\cos\theta_w}$	$\bar{e}_L e_R$ (g_2)	H
L_3^μ	0	1	0	1	1	$\frac{\cos\theta_w}{\sin\theta_w}$	$\bar{\nu}_L e_L$ $(\sqrt{2}g_3)$	W^+ W'^+
				0	0	0	$\bar{e}_L e_L$ $(-g_3)$ $\bar{\nu}_L \nu_L$ (g_3)	γ Z^0 Z'
				-1	-1	$-\frac{\cos\theta_w}{\sin\theta_w}$	$\bar{e}_L \nu_L$ $(\sqrt{2}g_3)$	W^- W'^-
L_1	2	0	1	0	1	$-\frac{\sin\theta_w}{\cos\theta_w}$	$e_L \nu_L$ $(-\lambda_1)$ (antisymm.)	
$\tilde{L}_1$	2	0	2	0	2	$-2\frac{\sin\theta_w}{\cos\theta_w}$	$e_R e_R$ $(\tilde{\lambda}_1)$ (symm.)	
L_2^μ	2	1	3/2	1/2	2	$-\frac{4\sin^2\theta_w - 1}{2\sin\theta_w\cos\theta_w}$	$e_R e_L$ (λ_2)	
				$-1/2$	1	$-\frac{2\sin^2\theta_w + 1}{2\sin\theta_w\cos\theta_w}$	$e_R \nu_L$ (λ_2)	
L_3	2	0	1	1	2	$-\frac{2\sin^2\theta_w - 1}{\sin\theta_w\cos\theta_w}$	$e_L e_L$ $(-\sqrt{2}\lambda_3)$	
				0	1	$-\frac{\sin\theta_w}{\cos\theta_w}$	$e_L \nu_L$ $(-\lambda_3)$ (symm.)	
				-1	0	$-\frac{1}{\sin\theta_w\cos\theta_w}$	$\nu_L \nu_L$ $(\sqrt{2}\lambda_3)$	

This provides clearer, but assumption dependent, information.

2.2.1 Flavour diagonal couplings

One of the simplest choices is a flavour diagonal coupling matrix with identical strength to all three flavours:

$$\lambda^{ij} = \lambda\delta^{ij} \equiv \lambda \begin{pmatrix} 1 & 0 & 0 \\ 0 & 1 & 0 \\ 0 & 0 & 1 \end{pmatrix} . \tag{4}$$

This may be natural for a gauge bilepton if there is no leptonic CKM matrix. It clearly does not apply to L_1, whose coupling matrix is antisymmetric. In this model, there are fewer low-energy constraints, because they usually originate from flavour changing processes.

2.2.2 Flavour democracy

Another possible Ansatz, which maximally mixes all three families, is inspired from a universal Yukawa interactions model [48]:

$$\lambda^{ij} \equiv \lambda \begin{pmatrix} 1 & 1 & 1 \\ 1 & 1 & 1 \\ 1 & 1 & 1 \end{pmatrix} . \tag{5}$$

For L_1, we will assume that the "flavour democratic" coupling matrix is of the form:

$$\lambda^{ij} \equiv \lambda \begin{pmatrix} 0 & 1 & 1 \\ -1 & 0 & 1 \\ -1 & -1 & 0 \end{pmatrix} . \tag{6}$$

This naturally leads to lepton flavour violating processes and the resulting bounds from low-energy experiments are rather strict.

2.2.3 Flavour infiltration

There is a mechanism that defines generations in approximately the same way as for u and d type quarks, with small CKM mixing angles. In [49], it was suggested that this "approximate flavour symmetry" may be a property of the low-energy effective theory derived from any extension of the standard model. In this case, the dilepton-lepton coupling matrix would be of the form

$$\lambda^{ij} \equiv \begin{pmatrix} \lambda^1 & \frac{m_e}{m_\mu}(\lambda^2 - \lambda^1) & \frac{m_e}{m_\tau}(\lambda^3 - \lambda^1) \\ \frac{m_e}{m_\mu}(\lambda^2 - \lambda^1) & \lambda^2 & \frac{m_\mu}{m_\tau}(\lambda^3 - \lambda^2) \\ \frac{m_e}{m_\tau}(\lambda^3 - \lambda^1) & \frac{m_\mu}{m_\tau}(\lambda^3 - \lambda^2) & \lambda^3 \end{pmatrix} . \tag{7}$$

This structure of the coupling matrix, which involves only three free parameters may be particularly appropriate for the scalar bileptons. We anti-symmetrize this matrix for L_1 (whose coupling matrix must be anti-symmetric in generation space) in the obvious way: we set the diagonal elements to zero, and put negative signs in front of the lower triangle.

2.3 Interactions with neutral gauge bosons

The interactions of the scalar and vector bileptons with the neutral gauge fields are described by the following lagrangians:

$$\mathcal{L}_{J=0} = (D_\mu L)^\dagger (D^\mu L) \tag{8}$$

$$\begin{aligned}\mathcal{L}_{J=1} = & -1/2(D_\mu L_\nu - D_\nu L_\mu)^\dagger (D^\mu L^\nu - D^\nu L^\mu) \\ & -i\kappa_\gamma e Q_\gamma L^\dagger_\mu L_\nu (\partial^\mu A^\nu - \partial^\nu A^\mu) \\ & -i\kappa_Z e Q_Z L^\dagger_\mu L_\nu (\partial^\mu Z^\nu - \partial^\nu Z^\mu) \ ,\end{aligned} \tag{9}$$

where L and L_μ denote generic scalar and vector bileptons. The covariant derivative is given by

$$D_\mu = \partial_\mu - ieQ_\gamma A_\mu - ieQ_Z Z_\mu \ . \tag{10}$$

The electric and weak charges Q_γ and Q_Z are uniquely determined by their hypercharge Y and weak isospin projection T_3

$$Q_\gamma = T_3 + Y \qquad Q_Z = T_3 \frac{\cos\theta_w}{\sin\theta_w} - Y \frac{\sin\theta_w}{\cos\theta_w} \ . \tag{11}$$

They are listed in Table 2.1 along with the other quantum numbers for all bileptons.

For the vector bileptons there is an extra complication due to our *a priori* ignorance of their gauge nature. If they are gauge bosons the *anomalous couplings* κ_γ and κ_Z in the lagrangian (9) vanish at tree level. Finite values of these two parameters would generate electric quadrupole and anomalous magnetic dipole moments of the bileptons. The *minimal couplings* are obtained for $\kappa_\gamma = \kappa_Z = 0$, whereas for Yang-Mills bileptons $\kappa_\gamma = \kappa_Z = 1$. For simplicity, we shall mostly focus on these two possibilities, *i.e.*, $\kappa = 0$ or $\kappa = 1$. Still, we keep in mind that in principle these parameters can take any value.

The bileptons may also have self-interactions or couplings to the Higgs or other unobserved particles. Such interactions can in some cases be important, for instance in generating neutrino masses or magnetic moments [4,6, 25,50]. We do not consider this complication here, as it involves the introduction of new free parameters describing the couplings between bileptons and other bosons. Without these interactions, the bileptons can only decay to a pair of leptons.

2.4 Mass eigenstates

Before proceeding further into any phenomenological analysis, it is important to note that the electroweak eigenstates we have just described may not be mass eigenstates, and that members of a given multiplet may not have the same mass. Those bileptons which carry the same spin and electromagnetic charge, *i.e.*, (L_1^-, L_3^-) and $(\tilde{L}_1^{--}, L_3^{--})$, could mix. In principle, if no particular model is referred to, the mixing angles remain free parameters. However the couplings of the gauge eigenstates to leptons $(\lambda_1, \tilde{\lambda}_1, \lambda_3)$ can easily be disentangled at colliders by partitioning into symmetric and antisymmetric couplings (for L_1^- and L_3^-) or with polarized experiments (for $\tilde{L}_1^{--}$ and L_3^{--}). We therefore shall not consider bilepton mixing, and we may use the couplings summarized in Table 2.1 as such.

The fact that members of a multiplet may not have the same mass is relevant for the low-energy bounds. If we assume that the bileptons acquire an $SU(2) \times U(1)$ invariant mass somewhere above the electroweak scale, then any mass splittings between members of an $SU(2)$ multiplet should be comparatively small. In this case, a bound on λ^2/m^2 for one member of a multiplet applies approximately to other members. We nonetheless list the bounds on multiplet members of different electric charge separately, because there is no absolute guarantee that the masses of $SU(2)$ multiplets are approximately degenerate.

3 Low-energy bounds

Low-energy bounds on the bileptons can be derived from the good agreement between theory and experiment in processes expected in the standard model, and from the non-observation of reactions which are forbidden or suppressed in the standard model. Following the Particle Data Book [51], which lists upper bounds on most branching ratios at 90% confidence level, we list our constraints "at 2 σ".

The mass of any $L = 2$ bileptons is constrained to exceed at least 38 GeV by LEP1 (see Sect. 4.1). This means that we can usually approximate the low-energy effects of bileptons in terms of four lepton operators. Details on how to derive the four fermion interactions are presented in Appendix A. The various renormalizable bilepton interactions and the four-fermion interactions that they induce are listed in Table 2. We will use these repeatedly throughout this section.

As previously discussed, we neglect the phases of the coupling constants. This means that for flavour non-diagonal processes the signs in front of the four-fermion vertices in Table 2 are irrelevant, and we neglect them. In the text, we generically compute bounds from each process on a four fermion vertex of specified tensor structure, but with arbitrary coefficient $a\lambda^2/m_L^2$. The factor "a" contains the possible factors of 2 and 1/2 (see Table 2). In the tables of results we list the bounds for each bilepton.

We compute bounds from muon physics in the first subsection, and from tau physics in the second. In the third subsection, we briefly list other constraints.

Table 2. Four fermion vertices induced by the $L = 2$ bileptons, in their original and Fierz-transformed standard model-like forms. The conversion is easily performed with the relations (A.3–A.5) of Appendix A. In the text we assume the couplings are real. Coupling constant indices in square brackets are antisymmetric and in curly brackets are symmetric

$\tilde{L}_1^{--}$	$\frac{\tilde{\lambda}_1^{\{ij\}}\tilde{\lambda}_1^{\{kl\}*}}{m_L^2}(\bar{e_i^c}P_R e_j)(\bar{e}_l P_L e_k^c)$	$\frac{1}{2}\frac{\tilde{\lambda}_1^{\{ij\}}\tilde{\lambda}_1^{\{kl\}*}}{m_L^2}(\bar{e_k}\gamma^\mu P_R e_i)(\bar{e}_l\gamma_\mu P_R e_j)$
L_1^-	$4\frac{\lambda_1^{[ij]}\lambda_1^{[kl]*}}{m_L^2}(\bar{e_i^c}P_L\nu_j)(\bar{\nu}_l P_R e_k^c)$	$2\frac{\lambda_1^{[ij]}\lambda_1^{[kl]*}}{m_L^2}(\bar{e_k}\gamma^\mu P_L e_i)(\bar{\nu}_l\gamma_\mu P_L\nu_j)$
$L_{2\mu}^{--}$	$\frac{\lambda_2^{ij}\lambda_2^{kl*}}{m_L^2}(\bar{e_i^c}\gamma^\mu P_R e_j)(\bar{e}_l\gamma_\mu P_R e_k^c)$	$-\frac{\lambda_2^{ij}\lambda_2^{kl*}}{m_L^2}(\bar{e_k}\gamma^\mu P_L e_i)(\bar{e}_l\gamma_\mu P_R e_j)$
$L_{2\mu}^-$	$\frac{\lambda_2^{ij}\lambda_2^{kl*}}{m_L^2}(\bar{\nu_i^c}\gamma^\mu P_R e_j)(\bar{e}_l\gamma_\mu P_R\nu_k^c)$	$-\frac{\lambda_2^{ij}\lambda_2^{kl*}}{m_L^2}(\bar{\nu_k}\gamma^\mu P_L\nu_i)(\bar{e}_l\gamma_\mu P_R e_j)$
L_3^{--}	$2\frac{\lambda_3^{\{ij\}}\lambda_3^{\{kl\}*}}{m_L^2}(\bar{e_i^c}P_L e_j)(\bar{e}_l P_R e_k^c)$	$\frac{\lambda_3^{\{ij\}}\lambda_3^{\{kl\}*}}{m_L^2}(\bar{e_k}\gamma^\mu P_L e_i)(\bar{e}_l\gamma_\mu P_L e_j)$
L_3^-	$4\frac{\lambda_3^{\{ij\}}\lambda_3^{\{kl\}*}}{m_L^2}(\bar{e_i^c}P_L\nu_j)(\bar{\nu}_l P_R e_k^c)$	$2\frac{\lambda_3^{\{ij\}}\lambda_3^{\{kl\}*}}{m_L^2}(\bar{e_k}\gamma^\mu P_L e_i)(\bar{\nu}_l\gamma_\mu P_L\nu_j)$
L_3^0	$2\frac{\lambda_3^{\{ij\}}\lambda_3^{\{kl\}*}}{m_L^2}(\bar{\nu_i^c}P_L\nu_j)(\bar{\nu}_l P_R\nu_k^c)$	$\frac{\lambda_3^{\{ij\}}\lambda_3^{\{kl\}*}}{m_L^2}(\bar{\nu_k}\gamma^\mu P_L\nu_i)(\bar{\nu}_l\gamma_\mu P_L\nu_j)$

3.1 Muon physics

There are two categories of constraints from muon physics. One can constrain the bileptons by requiring that their contributions to decay modes forbidden in the standard model (by lepton family number conservation) be less than the present experimental bounds. One can also require that bilepton contributions to allowed standard model processes be "sufficiently small". This gives a rough overall bound of $\lambda^2/m_L^2 \lesssim G_F$, that can in some cases be refined. For a clear (and entertaining) introduction to muon physics, see [52].

3.1.1 Polarized muon decay

The influence of the singly-charged vector bilepton L_2^μ on the decay of polarized muons has been discussed in [28]. If the four-fermion vertex mediating muon decay is a purely $(V-A)\times(V-A)$ effective interaction, then when a polarized muon decays at rest, the electron spectrum has a particular shape. If the effective vertex for the decay also contains, for instance, a sufficiently large $(V-A)(V+A)$ contribution, then this can be detected in the electron spectrum.

Following the notation of the Particle Data Book [51], we write the most general four fermion vertex for muon decay $\mu \to e\bar{\nu}_e\nu_\mu$, in terms of scalar, vector and tensor matrix elements for left-handed and right-handed electrons and muons. There are experimental upper bounds on the coefficient of each vertex, (except of course the SM $(V-A)\times(V-A)$ vertex, for which there is a lower bound). The coefficient g_{RR}^S of the vertex $2\sqrt{2}G_F(\bar{e}P_L\nu)(\bar{\nu}P_R\mu)$ is required to be less than .066 [53].

By Fierz rearranging, we have

$$(\bar{e}\gamma^\alpha P_R\mu)(\bar{\nu}_\mu\gamma_\alpha P_L\nu_e) = -2(\bar{e}P_L\nu_e)(\bar{\nu}_\mu P_R\mu)\ , \qquad (12)$$

so if $a\lambda^2/m_L^2$ is the coefficient of the $(V-A)(V+A)$ vertex (12), then

$$\frac{a\lambda^2}{m_L^2} < g_{RR}^S\sqrt{2}G_F \qquad (13)$$

or

$$a\lambda^2 < 1.1\left(\frac{m_L}{\text{TeV}}\right)^2\ . \qquad (14)$$

This applies to $L_{2\mu}^-$ and is listed in the tables as $\mu_R \to e\bar{\nu}\nu$.

3.1.2 The decay $\mu^- \to e^-\bar{\nu}_\mu\nu_e$

The muon decay $\mu^- \to e^-\bar{\nu}_\mu\nu_e$ has been considered in [29–31,37,38]. This lepton flavour violating process is forbidden in the standard model, but can be mediated at tree level by the singly-charged bileptons $L_{2\mu}^-$, L_3^- and L_1^- as depicted in Fig. 1. (Note that an $L = 2$ bilepton can only conserve flavour if it couples to a single generation of leptons; if it couples to multiple generations, its interactions can still be flavour diagonal, in the sense that leptons of the same flavour meet at a vertex, as in (4)). The experimental bound on the branching ratio (compared to ordinary muon decay) is B.R. $< 1.2\%$ [54]. We assume that this applies to $(V-A)(V+A)$ vertices as well as $(V-A)(V-A)$. There is also a bound from the ratio [20, 24]

$$\frac{\sigma(\bar{\nu}_\mu e^- \to \mu^-\bar{\nu}_e)}{\sigma(\nu_\mu e^- \to \mu^-\nu_e)} \leq .05 \qquad (15)$$

but we obtain a slightly better constraint from the decay:

$$\frac{a\lambda^2}{m_L^2} < \sqrt{.012}\times 2\sqrt{2}G_F \qquad (16)$$

or

$$a\lambda^2 < 3.6\left(\frac{m_L}{\text{TeV}}\right)^2\ . \qquad (17)$$

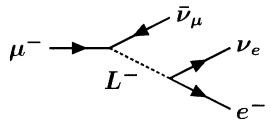

Fig. 1. Tree level process mediated by a singly-charged bilepton that could induce $\mu^- \to e^-\nu_e\bar{\nu}_\mu$ decays

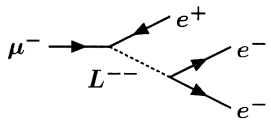

Fig. 2. Tree level process mediated by a doubly-charged bilepton that could induce $\mu^- \to e^-e^-e^+$ decays

The results are listed in Table 3 in Sect. 3.4. This combination of coupling constants will be better constrained by the KARMEN neutrino oscillation experiment (see Sect. 3.3.3).

3.1.3 The decay $\mu \to 3e$

The decay of a muon into three electrons has been discussed in [16,25,36]. This lepton flavour violating process is forbidden in the standard model, but can be mediated at tree level by the doubly-charged bileptons $L^{--}_{2\mu}$, L^{--}_3 and $\tilde{L}^{--}_1$ as depicted in Fig. 2. For $V \pm A$ bilepton vertices, the rate ought to be the same as for standard model muon decay (up to electron mass corrections), with $a\lambda^2/m_L^2$ substituted for $2\sqrt{2}G_F$. The upper bound on the branching ratio is 10^{-12} [55], so one has

$$\sqrt{2}\frac{a\lambda^2}{m_L^2} < \sqrt{10^{-12}} \times 2\sqrt{2}G_F \tag{18}$$

or

$$a\lambda^2 < 2.3 \times 10^{-5} \left(\frac{m_L}{\text{TeV}}\right)^2 . \tag{19}$$

The numerical bounds are given in Table 3, Sect. 3.4.

Note that this *does* bound 4-fermion vertices consisting of four fermions of the same chirality, although at first sight this seems to imply making two identical electrons at the same place. One can see in the original vertex (before Fierz rearrangement) that the two identical fermions do not multiply to zero, but rather induce a Feynman rule vertex $i2\lambda$. The rate in then divided by 2, for identical fermions in the final state, which gives the $\sqrt{2}$ on the left hand side of (18).

3.1.4 The decay $\mu \to e\gamma$

The radiative muon decay has been considered in [6,16,25, 38,56]. This lepton flavour violating process is forbidden in the standard model, but can be mediated at the one-loop level by the charged bileptons as depicted in Fig. 3. The branching ratio of this decay is constrained to be very small: $BR(\mu \to e\gamma) < 4.9 \times 10^{-11}$ [57]. However,

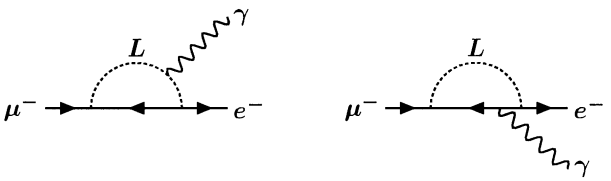

Fig. 3. One-loop diagrams mediated by doubly- or singly-charged bileptons that could induce $\mu \to e\gamma$

this is a one-loop process, so the matrix element is suppressed by a factor $\sim (1/4\pi)^2$. The decay $\mu \to 3e$ gives a stronger bound, but $\mu \to e\gamma$ applies to different combinations of generation indices, because one can have any lepton flavour in the loop.

The matrix element coupling two on-shell fermions to an on-shell photon can be written

$$\mathcal{M}[f_i(p_i) \to f_f(p_f) + \gamma(q)] = -i\bar{u}_f(p_f)\frac{\sigma^{\mu\nu}q_\nu}{m_i + m_f}\left[F_V(q^2) + F_A(q^2)\gamma_5\right]u_i(p_i) , \tag{20}$$

where $\sigma^{\mu\nu} \equiv \frac{-i}{2}[\gamma^\mu, \gamma^\nu]$ and $q^2 = 0$. The decay rate of f_i to $f_f + \gamma$ is

$$\Gamma(f_i \to f_f + \gamma) = \frac{m_i}{8\pi}\left[F_V^2(0) + F_A^2(0)\right] \leq 1.5\times10^{-29}\,\text{GeV} . \tag{21}$$

The magnetic ($F_V(0)$) and electric ($F_A(0)$) dipole moments are both finite, and $F_V \simeq F_A \equiv F$ for chiral fermions, so this gives

$$F \leq 4.2 \times 10^{-14} \tag{22}$$

for muon decay.

For scalar bileptons, we estimate the one-loop diagrams of Fig. 3 to be

$$F \simeq e\sum_k \left(\frac{Q_k}{12} - \frac{5Q_L}{12}\right)\frac{\lambda^{\mu k}\lambda^{ek}m_\mu^2}{(4\pi)^2 m_L^2} + \mathcal{O}\left(\frac{e\lambda^2 m_\mu^2 m_k^2}{(4\pi m_L^2)^2}\right) , \tag{23}$$

where Q_L and Q_k are the electric charges of the bilepton and the intermediate fermion. For vector bileptons, we estimate the leading order contribution from the one-loop diagrams of Fig. 3 to be

$$F \simeq e\sum_k \left(Q_k - \frac{3Q_L}{4}\right)\frac{\lambda^{\mu k}\lambda^{ek}m_\mu^2}{(4\pi)^2 m_L^2} + \mathcal{O}\left(\frac{e\lambda^2 m_\mu^2 m_k^2}{(4\pi m_L^2)^2}\right) . \tag{24}$$

We do not need to flip the chirality of the internal lepton, so we expect an even power of the internal fermion mass. Note that we have only estimated these matrix elements. The constraints are therefore only approximate, and could be missing factors of two.

Assuming there are no cancellations in the sum over internal leptons, the leading order contribution in (23,24) dominates. For the scalar bileptons the approximate bound is then

$$aQ_L\sum_k \lambda^{\mu k}\lambda^{ek} \lesssim 4 \times 10^{-3}\left(\frac{m_L}{\text{TeV}}\right)^2 \tag{25}$$

where $a = 2$ if a pair of identical fermions meet at a vertex, and 1 otherwise. The bound on the couplings of the vector is of order

$$\left(Q_k - \frac{3Q_L}{4}\right) \sum_k \lambda^{\mu k}\lambda^{ek} \lesssim 2 \times 10^{-3} \left(\frac{m_L}{\text{TeV}}\right)^2 . \quad (26)$$

Ignoring the sum over the internal fermions in (23) and (24) implies that the bound on the sum is similar to the bound on the elements of the sum. This is a non-trivial assumption; we do not expect this to be the case for gauge vector bosons (for instance), whose coupling matrices should be unitary. If, for any of the bileptons, the coupling matrices are unitary ($\sum_k \lambda^{\mu k}\lambda^{ek*} = 0$), then the bounds we quote are overly optimistic, and the first non-zero contribution to $\mu \to e\gamma$ is of order

$$\frac{\lambda^2}{(4\pi)^2}\frac{m_\mu^2 m_k^2}{m_L^4} . \quad (27)$$

This does not give interesting bounds on the bileptons. We therefore quote in the summary Table 3 the "non-GIM-suppressed" bounds, while noting that they only apply to bileptons whose coupling matrices are not unitary. We explicitly consider the sum when we focus on specific models in Tables 5–7.

The product of couplings $\lambda^{\mu e}\lambda^{ee}$ is better constrained by the $\mu \to 3e$ reaction. In Tables 3 and 4, we quote bounds on $\lambda^{\mu\mu}\lambda^{\mu e}$ and $\lambda^{\mu\tau}\lambda^{\tau e}$ assuming that the lowest order contributions with different fermions in the loop do not cancel against each other. As discussed in the previous paragraph, this may not be a valid assumption.

As noted in [56], under certain circumstances two-loop diagrams may give better bounds on the $SU(2)$ triplet bileptons than the one-loop diagrams we have considered. This happens if the scalar develops a vacuum expectation value and couples to the W bosons; as we explicitly ignore this possibility, the one-loop diagram should dominate.

3.1.5 $g-2$ of the muon

The anomalous magnetic moment of the electron and the muon are two of the most accurately measured quantities in physics, and are frequently used to constrain new particles. The measured value of $(g-2)_\mu$ is [51]

$$\frac{(g-2)_\mu}{2} = [116592300 \pm 840] \times 10^{-11} \quad (28)$$

and the standard model prediction [58] is $(g-2)_\mu^{th} = 116591739 \pm 154 \times 10^{-11}$. This allows, at two σ, a new physics contribution of order

$$\delta\left(\frac{g-2}{2}\right) \simeq 170 \times 10^{-10} \quad (29)$$

The contribution to $g-2$ of the muon from bileptons, or generic bosons from beyond the standard model, has been computed in [16,19,22,27,30,31,36,38,59].

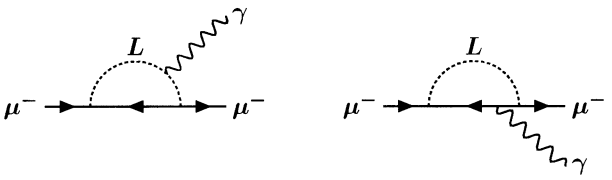

Fig. 4. One-loop diagrams mediated by doubly- or singly-charged bileptons that could contribute to $g-2$

As we shall see, these constraints are not particularly strong; we list them anyway, because unlike most low energy bounds, $(g-2)/2$ constrains the square of a coupling constant.

For the doubly-charged bileptons, both diagrams in Fig. 4 contribute; for singly-charged bileptons, the photon does not couple to the internal neutrino. These diagrams have been evaluated in [60,59], from which we can read off the leading order contributions.

If the bilepton is a vector boson, then the contribution to $(g-2)_\mu$ is

$$\left(\frac{2Q_f}{3} - \frac{5Q_L}{6}\right)\frac{h^2 m_\mu^2}{8\pi^2 m_L^2} \quad (30)$$

In these expressions and those that follow for scalar bileptons, h is the coupling constant appearing at the bilepton-lepton-lepton vertex. It can be read off from (3), providing one remembers to include a factor of 2 at the vertices where L_1^{--} and L_3^{--} meet two identical fermions. For scalar bileptons, the contribution os

$$\left(\frac{Q_L}{12} - \frac{Q_f}{6}\right)\frac{h^2 m_\mu^2}{8\pi^2 m_L^2} . \quad (31)$$

From (29), this gives bounds of order

$$\lambda^2 < 100 \left(\frac{m_L}{\text{TeV}}\right)^2 \quad (32)$$

for the vector bileptons, and of order

$$\lambda^2 < 500 \left(\frac{m_L}{\text{TeV}}\right)^2 \quad (33)$$

for the scalars. The exact bounds are listed in Tables 3 and 4. As noted earlier, these bounds are weak, but apply to coupling constant combinations $|\lambda^{\mu j}|^2$. The bounds on bileptons from $g-2$ for the electron are too weak to be interesting, because the contributions are suppressed by the electron mass squared.

3.1.6 Muonium-antimuonium conversion

Doubly-charged bileptons with flavour diagonal couplings may mediate the conversion of μ^+e^- atoms (muonium) into μ^-e^+ atoms (antimuonium) as depicted in Fig. 5. This has been considered by many people [12,16,19,20,25, 27,30–33,37]; [31] also studied muonium hyperfine splitting and [32] have studied this in a magnetic field.

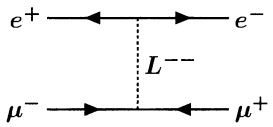

Fig. 5. Muonium-antimuonium conversion mediated at tree-level by doubly-charged bileptons

As yet no such events have been observed and the most stringent 90% C.L. experimental bounds on the effective $V \pm A$ interactions are [61]

$$\frac{a\lambda^2}{m_L^2} < \begin{cases} 0.018 \times 2\sqrt{2}G_F & \text{for } (V \pm A)(V \pm A) \text{ vertices} \\ 0.012 \times 2\sqrt{2}G_F & \text{for } (V \pm A)(V \mp A) \text{ vertices} \end{cases} \tag{34}$$

or

$$a\lambda^2 < \begin{cases} 0.6 \left(\frac{m_L}{\text{TeV}}\right)^2 & \text{for } (V \pm A)(V \pm A) \text{ vertices} \\ 0.4 \left(\frac{m_L}{\text{TeV}}\right)^2 & \text{for } (V \pm A)(V \mp A) \text{ vertices .} \end{cases} \tag{35}$$

In the case of scalar bilepton exchange, these are identical fermions at the vertices, so the effective four-fermion vertex is multiplied by 4.

3.1.7 G_F from muon decay

Bilepton effects on the measurement of the Fermi constant have been mentioned in [16], and discussed in [6,31]. G_F is measured in muon decay to be $G_\mu = 1.16639(2) \times 10^{-5}$ [51]. This is then used to determine V^{ud} in neutron β decay. As discussed in [62], one can constrain new physics by comparing these leptonic and hadronic determinations of G. The bileptons could contribute at tree level to muon decay, and make the experimental determination of G_μ larger or smaller than its "true" value G_β that enters into β decay. We assume that the bileptons are the only new physics present, so G_β has the standard model value, and the CKM matrix is unitary.

It is clear that

$$G_\mu V_{ex} = G_\beta V_t \tag{36}$$

where V_{ex} is the experimental determination of a CKM angle, derived using G_μ for G_F, and V_t is the "true" CKM matrix element. Unitarity implies that

$$1 = \sum_i |V_t^{ui}|^2 \tag{37}$$

or, substituting from (36) and rearranging

$$\frac{G_\beta^2}{G_\mu^2} = \sum_i |V_{ex}^{ui}|^2 \tag{38}$$

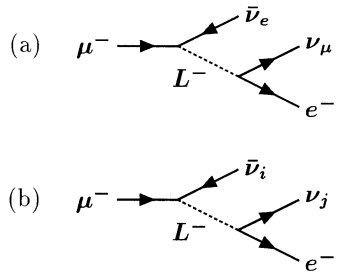

Fig. 6. a Tree level process mediated by a singly-charged bilepton that could interfere with the standard model process $\mu^- \to e^- \nu_e \bar{\nu}_\mu$. **b** Pure bilepton contribution to $\mu \to e\bar{\nu}\nu$ (the neutrino flavours are arbitrary)

The experimental measurements of V_{ui} in the Particle Data Book [51], at two sigma, imply

$$\sum_i |V_{ex}^{ui}|^2 = .9981 \pm .0055 \tag{39}$$

Setting $2\sqrt{2}G_\mu = 2\sqrt{2}G_\beta \pm a\lambda^2/m_L^2$, we obtain

$$-.0036 < \frac{aS\lambda^2}{\sqrt{2}G_\beta m_L^2} + \frac{a^2\lambda^4}{8G_\beta^2 m_L^4} < .0074 \tag{40}$$

Note that we are allowing for interference between the W and the bilepton; S is a possible chiral suppression factor that arises if the bilepton produces a right-handed rather than a left-handed electron. One needs to flip the electron chirality to interfere this amplitude with the standard model one, so $S = m_e/m_\mu$ [63]. (See the section on G_F measured in τ decays for a discussion of this, and more complete references.) This gives

$$-.059 \left(\frac{m_L}{\text{TeV}}\right)^2 < aS\lambda^2 < .12 \left(\frac{m_L}{\text{TeV}}\right)^2 \tag{41}$$

for the interference term, and

$$|a\lambda^2| < 2.8 \left(\frac{m_L}{\text{TeV}}\right)^2 \tag{42}$$

for the pure bilepton contribution.

The interference bound (41) is very strong, because it is a bound on $G_F\lambda^2/m_L^2$, rather than λ^4/m_L^4, and unitarity is satisfied at the $\sim .1$ % level. It applies to the scalar bileptons L_1^- and L_3^-. with $(V-A)(V-A)$ vertices for the couplings mediating the decay of a μ_L^- to an e_L^-, a ν_μ and a $\bar{\nu}_e$. This is a flavour non-diagonal process, where the μ_L^- meets the $\bar{\nu}_e$ at the same vertex, as shown in Fig. 6a.

The bound on the purely bileptonic contribution (42) constrains bilepton decays to any flavour of neutrino, as illustrated in Fig. 6b. The $(V + A)(V - A)$ vertices mediated by the vector bilepton $L_{2\mu}^-$, who suffer the helicity suppression factor $S = m_e/m_\mu$, are better constrained by the pseudoscalar matrix element constraint (14).

3.1.8 The weak mixing angle

Bilepton effects on the measurement of $\sin^2\theta_W$ have been considered in [38]. The weak mixing angle is measured on

the Z^0 resonance to be .2256±.0023 (on-shell scheme), and is measured leptonically at low E in the ratio of $\nu_\mu e \to \nu_\mu e$ to $\bar{\nu}_\mu e \to \bar{\nu}_\mu e$ to be .224 ±.009. Bileptons would contribute at tree level to the low-energy determination of $\sin^2\theta_W$, and very little to the LEP measurement, because LEP runs at the Z^0 peak. Bounds on bileptons from $\nu_e e \to \nu_e e$ have also been calculated [29]; these are similar to this, but constrain a different combination of generation indices, and will be discussed in Sect. 3.3.3.

Following the Particle Data Book notation, we write the neutrino–electron 4-fermion vertex in the form

$$2\sqrt{2}G_F(\bar{\nu}\gamma^\mu P_L\nu)(\bar{e}\gamma_\mu[g_L P_L + g_R P_R]e) \ , \qquad (43)$$

where $g_L = \frac{1}{2}(g_V - g_A), g_R = \frac{1}{2}(g_V + g_A)$. In the standard model one has at tree level $g_L = \sin^2\theta_W - 1/2, g_R = \sin^2\theta_W$. Using the standard model tree level values for g_L and g_R, and $\delta g_{L,R} = a\lambda^2/(2\sqrt{2}G_F m_L^2)$, the bound

$$\delta_{L,R} < 0.2256 - (0.224 - 0.018) \qquad (44)$$

gives

$$|a\lambda^2| < 0.65\left(\frac{m_L}{\mathrm{TeV}}\right)^2 \qquad (45)$$

for $L_{2\mu}^-$, L_1^- and L_3^-. These are bounds on the interference between the standard model and bilepton amplitudes, so they apply to bilepton vertices involving e, $\bar{e}$, ν_μ and $\bar{\nu}_\mu$.

3.2 Tau physics

The τ mass and branching ratios have recently been measured very accurately [64], and the new determinations are consistent within errors with the standard model. The bounds on new physics that can be derived from them have been thoroughly and clearly discussed in [44]. Here, we make a more cursory analysis, but include other rare decay bounds.

3.2.1 G_F from tau decay

The decays $\tau \to \ell\bar{\nu}\nu$ are observed at the expected standard model rate, which can be used to constrain bileptons by requiring that their contributions to G_F as measured in τ decays ($\equiv G_\tau$) be sufficiently small. The neutrino flavour is unobserved, so assuming that all the neutrinos are light, we can use this decay to bound bilepton-mediated decays to arbitrary neutrino flavours.

We assume that there is no new physics in the strongly interacting sector, so the CKM matrix is unitary, and G_F in β decay measures the four-fermion vertex induced by the standard model W. From our previous discussion of the bilepton contribution to G in muon decay, we know that at two sigma

$$\frac{G_\beta}{\hat{G}_\mu} = 1.0000 + .0018 - .0037 \qquad (46)$$

where (see [44,63] for a complete analysis)

$$\hat{G}_\mu^2 \simeq G_\mu^2(1 + 2g_{RR}^S\frac{m_e}{m_\mu}) \qquad (47)$$

In our analysis of muon decay, we assumed that $G_\mu = \hat{G}_\mu$, because g_{RR}^S in muon decay is better constrained by the shape of the electron spectrum than by the size of G. (Recall that $\sqrt{2}g_{RR}^S G$ was the coefficient of the $(V + A)(V - A)$ four fermion vertex (12)). Equation (47) is a linear approximation; g_{RR}^S appears unsquared because it is multiplied by the standard model vector coupling $g_{LL}^V \simeq 1$.

Recent τ data [64] implies, at one sigma,

$$\frac{\hat{G}_{e\tau}}{\hat{G}_\mu} = .999 \pm .003 \qquad (48)$$

and

$$\frac{\hat{G}_{e\tau}}{\hat{G}_{\mu\tau}} = 1.001 \pm .004 \qquad (49)$$

where $G_{\ell\tau}$ is G determined from $\tau \to \ell\nu\bar{\nu}$ assuming a $(V - A) \times (V - A)$ vertex.

Adding the errors in these "ratios of G" in quadrature, we obtain at two sigma:

$$\frac{\hat{G}_{e\tau}}{G_\beta} = 1.000 \pm .007 \qquad (50)$$

and

$$\frac{\hat{G}_{\mu\tau}}{G_\beta} = 1.000 \pm .009 \qquad (51)$$

Alternatively, we could have constrained the ratio of [G that bileptons contribute to at tree level]/[G that bileptons do not contribute to at tree level] from the ratio $G_{\ell\tau}/G_{\pi,K}$. $G_{\ell\tau}$ is G determined from leptonic τ decays, and $G_{\pi,K}$ is G determined from $\tau \to \pi\nu\bar{\nu}$ and $\tau \to K\nu\bar{\nu}$. The error in this ratio is also of order 1-2% [44,64], so it gives the same constraints.

Bileptons can induce two types of four fermion vertices that mediate tau decay: either $(\bar{\ell}\gamma^\mu R\tau)(\bar{\nu}\gamma_\mu L\nu)$ or $(\bar{\ell}\gamma^\mu L\tau)(\bar{\nu}\gamma_\mu L\nu)$. If the right-handed vertex is present, then we have

$$\hat{G}_{\ell\tau}^2 = G_\beta^2\left(1 + \frac{2a\lambda^2}{\sqrt{2}m_L^2 G}\frac{m_\ell}{m_\tau} + \frac{a^2\lambda^4}{8m_L^4 G^2}\right) \qquad (52)$$

which implies, from the standard model-bilepton interference term, that

$$a\lambda^{32}\lambda^{23} < 1.9\left(\frac{m_L}{\mathrm{TeV}}\right)^2 \qquad (53)$$

If bileptons induce the four-fermion vertex $(\bar{\ell}\gamma^\mu L\tau)$ $(\bar{\nu}_\tau\gamma_\mu L\nu_\ell)$ then $\hat{G}$ would be

$$\hat{G}_{\ell\tau} = G_\beta\left(1 + \frac{a\lambda^2}{2\sqrt{2}m_L^2 G}\right) \qquad (54)$$

which gives the bound

$$a\lambda^{31}\lambda^{13} < .23\left(\frac{m_L}{\text{TeV}}\right)^2, \quad a\lambda^{32}\lambda^{23} < .32\left(\frac{m_L}{\text{TeV}}\right)^2 \quad (55)$$

on the singly-charged scalar bileptons L_1^- and L_3^-, if the final states are such that there are interferences with the standard model amplitudes. For non-standard model processes similar to those depicted in Fig. 6 the bounds are

$$a\lambda^{\nu 3}\lambda^{\nu' 1} < 2.7\left(\frac{m_L}{\text{TeV}}\right)^2, \quad a\lambda^{\nu 3}\lambda^{\nu' 2} < 3.3\left(\frac{m_L}{\text{TeV}}\right)^2 \quad (56)$$

for both $(V+A)(V-A)$ and $(V-A)(V-A)$ vertices.

3.2.2 Lepton flavour violating tau decays

There are also tau lepton bounds from the non-observation of the flavour-changing decays $\tau \to \ell\gamma$, and $\tau \to 3\ell$ [65–67]. Here (and in the tables) ℓ means μ or e, and f is any charged lepton or antilepton (so 3ℓ is some $Q=0$ combination of muons and electrons). The bounds are straightforward copies of the muon calculations, and the results are listed in the tables. The experimental upper bounds on the τ branching ratios imply

$$F(\tau \to e\gamma) \lesssim 2.4 \times 10^{-8} \quad (57)$$

$$F(\tau \to \mu\gamma) \lesssim 4.0 \times 10^{-8} \quad (58)$$

which give bounds of order

$$Q\lambda^{\tau k}\lambda^{ek} < 8\left(\frac{m_L}{\text{TeV}}\right)^2 \quad (59)$$

$$Q\lambda^{\tau k}\lambda^{\mu k} < 13\left(\frac{m_L}{\text{TeV}}\right)^2 . \quad (60)$$

We have approximated $F_V \simeq F_A \equiv F$ as for the decay $\mu \to e\gamma$. We assume that the bilepton coupling matrices λ are not unitary, so that their contribution to $\tau \to \ell\gamma$ is not zero at lowest order (see the discussion following (24)).

The $\tau \to 3\ell$ decays imply

$$a\lambda^2 < .18\left(\frac{m_L}{\text{TeV}}\right)^2 \quad (61)$$

for the bileptons $L_{2\mu}^{--}, \tilde{L}_1^{--}$ and L_3^{--}. For simplicity, we conservatively neglect factors of 2 for identical fermions in these bounds.

3.3 Other physics

3.3.1 Compositeness searches

Constraints on bileptons from Bhabha scattering ($e^+e^- \to e^+e^-$) have been calculated in [27,29,34,68]. However, bounds on four fermion operators of the form $(\bar{e}\Gamma e)(\bar{f}\Gamma f)$ (f here is an e, μ or τ) have been calculated by the JADE and TASSO collaborations from PETRA data [69,70], and it is these stronger constraints that we quote.

It was pointed out in [71] that composite theories would produce effective four fermion vertices of the form

$$\begin{aligned}&\frac{g^2\eta_{LL}}{2\Lambda^2}(\bar{\psi}\gamma^\mu P_L\psi)(\bar{\psi}\gamma_\mu P_L\psi)\\ &\quad + \frac{g^2\eta_{RR}}{2\Lambda^2}(\bar{\psi}\gamma^\mu P_R\psi)(\bar{\psi}\gamma_\mu P_R\psi)\\ &\quad + \frac{g^2\eta_{RL}}{\Lambda^2}(\bar{\psi}\gamma^\mu P_R\psi)(\bar{\psi}\gamma_\mu P_L\psi) \quad (62)\end{aligned}$$

between the charged fermions. Including these interactions in the cross-section for $e^+e^- \to e^+e^-, \mu^+\mu^-, \tau^+\tau^-$ changes the angular distribution of the final state particles. For $g^2 \simeq 4\pi$, and $\eta_{PP'} = \pm 1$, JADE and TASSO give bounds on Λ between $1-7$ TeV [69,70]. The exact numbers depend on the sign and indices of η. Unfortunately, η_{LR}, does not seem to have been explicitly considered, so we assume the bound on Λ in this case to be $\simeq 3$ TeV. The exact constraints are in the tables, but are roughly

$$a\lambda^2 \le \frac{2\pi m_L^2}{\Lambda^2} \simeq .7\left(\frac{m_L}{\text{TeV}}\right)^2 \quad (63)$$

Four fermion operators at LEP and SLC have been discussed in [72], who show that experiments running on the Z peak do not provide strong generic bounds on four-fermion operators.

3.3.2 Neutrino oscillations

Bileptons can be constrained by neutrino oscillation experiments if the neutrinos are produced leptonically (in the decay of a muon). In this case, the bileptons could contribute at tree level to the production of the neutrino beam, but are unimportant in the detection of the neutrinos, because the cross section to scatter off an electron in the target is suppressed with respect to the cross section on nuclei by a factor of order m_e/E_ν. (Recall that bileptons do not couple to quarks.) See [73] for a thorough discussion of constraints on various kinds of new physics from neutrino oscillation experiments.

As usual, we assume that bileptons are the only source of physics beyond the standard model. They can mediate at tree level the decays $\mu \to e\nu_i\bar{\nu}_j$ where $i \neq \mu$. The neutrino oscillation experiment bounds on $P_{\mu i} = \frac{1}{2}\sin^2 2\theta$ for large Δm^2 are upper limits on the probability of making an i neutrino when one expected a μ neutrino. Most of these flavour oscillation limits are of order $1-10\%$, and therefore imply weaker limits than can be derived from unitarity arguments (Sect. 3.1.6). However, as noted in [73], the bounds from the KARMEN experiment [74] on $\nu_\mu \to \nu_e$ oscillations and the FNAL E351 experiment [75] on $\nu_\mu \to \nu_\tau$ give

$$\begin{aligned}P_{\mu e} &< 3 \times 10^{-3} \quad (64)\\ P_{\mu\tau} &< 2 \times 10^{-3} ,\end{aligned}$$

which translates into the bound

$$\frac{a\lambda^2}{m_L^2} < \sqrt{P_{\mu i}} \times 2\sqrt{2}G_F \quad (65)$$

or

$$a\lambda^2 \lesssim 1.8 \left(\frac{m_L}{\text{TeV}}\right)^2 \text{ oscillation to electrons} \quad (66)$$

$$a\lambda^2 \lesssim 1.5 \left(\frac{m_L}{\text{TeV}}\right)^2 \text{ oscillation to taus .} \quad (67)$$

This constraint applies to a bilepton vertex involving a μ, $\bar{e}$, ν_f (f is arbitrary) and a $\bar{\nu}_e$ or a $\bar{\nu}_\tau$. Although the experimental results are very precise, the ensuing bounds are not particularly strong because there is no enhancement via interferences with a standard model amplitude.

3.3.3 Neutrino scattering

The elastic scattering of neutrinos off electrons is in principle a good place to look for generation diagonal bounds on bileptons, but unfortunately the event rate is rather low. Constraints from neutrino scattering processes on vector bileptons were considered in [29].

The $\nu_e e$ scattering cross-section in the presence of right-handed neutrinos and an arbitrary four fermion vertex was derived in [76]. Assuming that our neutrinos are left-handed, the vertex can be written in terms of the effective coupling constants $g_L = g_L^{SM} + \delta g_L$ and $g_R = g_R^{SM} + \delta g_R$ (see Sect. 3.1.7). These were measured in $\nu_e e$ scattering at LAMPF [77], to be [78]

$$g_R^2 = .534 \pm .184 \quad (68)$$
$$g_L^2 = .084 \pm .031 \ .$$

Using the LEP determination of $\sin^2\theta_W$, we get the two sigma bounds

$$a\lambda^2 < 7 \left(\frac{m_L^2}{\text{TeV}}\right)^2 \quad (69)$$

for the singly-charged bileptons.

3.3.4 Limits from neutrino masses and magnetic moments

We have looked for possible bounds on bileptons from neutrino magnetic moments, but did not find anything useful. We do not find bounds from neutrino masses, because we assume that lepton number is conserved, and that there are no right-handed neutrinos.

3.4 Low-energy summary

In an attempt to clarify what ranges of bilepton mass and coupling constant are allowed, we present the constraints in various ways. We first simply list the bounds in Table 3 and 4. This is not very appealing, but does contain model-independent information. We then make various assumptions about the relative magnitudes of the different entries in the coupling constant matrices λ^{ij}, as described in Sect. 2.2. This allows us to present attractive (but assumption dependent) constraints in Tables 5, 6 and 4.

In Tables 3 and 4, we list the numerical bounds on λ^2/m_L^2 in units of TeV^{-2} for each bilepton from the various low-energy processes we have considered. We list bounds separately for each member of the bilepton multiplets, to allow different members of an $SU(2)$ multiplet to have different masses. We assume, in computing these bounds, that the bilepton is the only addition to the standard model but we make no assumptions about the structure of the coupling constant matrices.

The bounds listed in Tables 3 and 4 are difficult to interpret. There are rarely constraints on squares coupling constant products of the form $|\lambda^{ij}|^2$. Rather, the bounds are usually on the products $\lambda^{ij}\lambda^{kl}$ with $i \neq k, j \neq l$. There are two reasons for this. Firstly, a number of constraints come from the non-observation of lepton flavour violating interactions that are forbidden in the standard model and usually these are not mediated by generation diagonal bilepton couplings. The second difficulty is that most of the data come from decays, which involve leptons of different flavours for kinematic reasons. This means, for example, that if there was a ~ 100 GeV boson with gauge strength coupling only to muons or only to taus, we would not have seen it.

In Table 5, we assume flavour diagonal interactions (4). This might be a reasonable coupling constant matrix for a gauge bilepton, in the limit of massless neutrinos, *i.e.*, in the absence of a leptonic CKM matrix. The doubly-charged bileptons are best constrained by the absence of muonium oscillations, whereas the singly-charged ones by neutrino oscillation experiments and muon decay. New neutrino oscillation data could improve these bounds.

In Table 6, we list the best constraint on each coupling constant assuming flavour democracy (5). The doubly-charged bileptons are best constrained by the non-observation of $\mu \to 3e$ decays, whereas the singly-charged ones by radiative muon decays.

Assuming flavour infiltration (7), we list in Table 7 the upper bounds on λ^1, λ^2 and λ^3. To compute bounds on the parameter λ^1 (for example), from a decay involving $\lambda^{12}\lambda^{11}$, we set $\lambda^{12} \simeq \frac{m_e}{m_\mu}\lambda^1$. If $\lambda^2 < \lambda^1$, this is a good approximation, and if $\lambda^2 > \lambda^1$, it gives conservative bounds. The strongest bounds originate from the non-observation of $\mu \to 3e$ decays and radiative muon and tau decays.

To gauge the sensitivity of the low-energy experiments, recall that the coefficient of the W mediated standard model 4 fermion vertex is $2\sqrt{2}G_F$, which, in our notation, would correspond to $\lambda \simeq 6m_L/\text{TeV}$. The standard model Yukawa couplings for leptons are of order $10^{-7} \to 10^{-2}$. One can see from Tables 7 and 5 that if one makes reasonable assumptions about the coupling constant matrix λ, bileptons with masses ~ 100 GeV $\to 10$ TeV are consistent with low-energy data.

4 High-energy bounds

Since bileptons do not couple to quarks, the ideal high-energy setup for their discovery seems to be a lepton and/or photon collider. Nevertheless, the Drell-Yan bilepton

Table 3. Summary of the low-energy constraints on the bilepton-lepton-lepton coupling λ from experiments involving muons. The bilepton mass is given in units of 1 TeV. The bounds are only for absolute values of the couplings. The bounds on the L_2^μ couplings apply as well to the symmetrized combinations. The labels ℓ stand for e or μ, whereas the labels f stand for all three families. The $g-2$ bounds on λ_1 and λ_3 should be divided by 4 for $f=2$; the $\mu \to e\gamma$ bounds on λ_1 and λ_3 should be divided by 2 for $f=1,2$. Both the $g-2$ and $\mu \to e\gamma$ bounds apply to a sum of coupling constant products; we assume there are no cancellations between terms in these bounds

experiment	$\tilde{L}_1^{--}$	L_1^-	$L_{2\mu}^{--}$	$L_{2\mu}^-$	L_3^{--}	L_3^-
$\mu_R \to e\bar{\nu}\nu$				$\frac{\lambda^{1f}\lambda^{2f'}}{m_L^2} < 1\times10^{-0}$		
$\mu_L \to e\bar{\nu}_\mu\nu_e$				$\frac{\lambda^{11}\lambda^{22}}{m_L^2} < 4\times10^{-0}$		$\frac{\lambda^{11}\lambda^{22}}{m_L^2} < 5\times10^{-1}$
G_μ		$\frac{\lambda^{[12]}\lambda^{[21]}}{m_L^2} < 6\times10^{-2}$				$\frac{\lambda^{12}\lambda^{21}}{m_L^2} < 6\times10^{-2}$
		$\frac{\lambda^{[1f]}\lambda^{[2f']}}{m_L^2} < 1\times10^{-0}$		$\frac{\lambda^{1f}\lambda^{2f'}}{m_L^2} < 3\times10^{-0}$		$\frac{\lambda^{1f}\lambda^{2f'}}{m_L^2} < 1\times10^{-0}$
$\sin^2\theta_w$		$\frac{\lambda^{[12]}\lambda^{[12]}}{m_L^2} < 3\times10^{-1}$		$\frac{\lambda^{12}\lambda^{12}}{m_L^2} < 6\times10^{-1}$		$\frac{\lambda^{12}\lambda^{12}}{m_L^2} < 3\times10^{-1}$
$\mu \to ee\bar{e}$	$\frac{\lambda^{11}\lambda^{12}}{m_L^2} < 5\times10^{-5}$		$\frac{\lambda^{11}\lambda^{12}}{m_L^2} < 2\times10^{-5}$		$\frac{\lambda^{11}\lambda^{12}}{m_L^2} < 2\times10^{-5}$	
$\mu \to e\gamma$	$\frac{\lambda^{f2}\lambda^{f1}}{m_L^2} < 2\times10^{-3}$	$\frac{\lambda^{[f2]}\lambda^{[f1]}}{m_L^2} < 4\times10^{-3}$	$\frac{\lambda^{f2}\lambda^{f1}}{m_L^2} < 2\times10^{-3}$	$\frac{\lambda^{f2}\lambda^{f1}}{m_L^2} < 2\times10^{-3}$	$\frac{\lambda^{f2}\lambda^{f1}}{m_L^2} < 1\times10^{-3}$	$\frac{\lambda^{f2}\lambda^{f1}}{m_L^2} < 2\times10^{-3}$
$M \leftrightarrow \bar{M}$	$\frac{\lambda^{11}\lambda^{22}}{m_L^2} < 3\times10^{-1}$		$\frac{\lambda^{11}\lambda^{22}}{m_L^2} < 4\times10^{-1}$		$\frac{\lambda^{11}\lambda^{22}}{m_L^2} < 2\times10^{-1}$	
$(g-2)_\mu$	$\frac{\lambda^{f2}\lambda^{f2}}{m_L^2} < 4\times10^{+2}$	$\frac{\lambda^{[f2]}\lambda^{[f2]}}{m_L^2} < 1\times10^{+3}$	$\frac{\lambda^{f2}\lambda^{f2}}{m_L^2} < 5\times10^{+1}$	$\frac{\lambda^{f2}\lambda^{f2}}{m_L^2} < 1\times10^{+2}$	$\frac{\lambda^{f2}\lambda^{f2}}{m_L^2} < 4\times10^{+2}$	$\frac{\lambda^{f2}\lambda^{f2}}{m_L^2} < 1\times10^{+3}$

Table 4. Summary of the low-energy constraints on the bilepton-lepton-lepton coupling λ from τ decays, compositeness searches and neutrino experiments. The bilepton mass is given in units of 1 TeV. The bounds are only for absolute values of the couplings. The bounds on the L_2^μ couplings apply as well to the symmetrized combinations. The labels ℓ stand for e or μ, whereas the labels f stand for all three families. The $\tau \to \ell\gamma$ bounds apply to a sum of coupling constant products; we assume there are no cancellations between terms in these bounds. (The bounds on L_1^{--} and L_3 with arbitrary indices f and/or ℓ should be divided by 2 (or 4) if one (or both) of the λ is flavour diagonal)

experiment	$\tilde{L}_1^{--}$	L_1^-	$L_{2\mu}^{--}$	$L_{2\mu}^-$	L_3^{--}	L_3^-
G_τ		$\frac{\lambda^{[3f]}\lambda^{[\ell f']}}{m_L^2} < 2\times10^{-0}$		$\frac{\lambda^{3f}\lambda^{\ell f}}{m_L^2} < 3\times10^{-0}$		$\frac{\lambda^{3f}\lambda^{\ell f'}}{m_L^2} < 2\times10^{-0}$
		$\frac{\lambda^{[32]}\lambda^{[23]}}{m_L^2} < 2\times10^{-1}$		$\frac{\lambda^{32}\lambda^{23}}{m_L^2} < 2\times10^{-0}$		$\frac{\lambda^{32}\lambda^{23}}{m_L^2} < 2\times10^{-1}$
		$\frac{\lambda^{[31]}\lambda^{[13]}}{m_L^2} < 1\times10^{-1}$				$\frac{\lambda^{31}\lambda^{13}}{m_L^2} < 1\times10^{-1}$
$\tau \to 3\ell$	$\frac{\lambda^{3\ell}\lambda^{\ell'\ell''}}{m_L^2} < 4\times10^{-1}$		$\frac{\lambda^{3\ell}\lambda^{\ell'\ell''}}{m_L^2} < 2\times10^{-1}$		$\frac{\lambda^{3\ell}\lambda^{\ell'\ell''}}{m_L^2} < 2\times10^{-1}$	
$\tau \to e\gamma$	$\frac{\lambda^{f3}\lambda^{f1}}{m_L^2} < 4\times10^{-0}$	$\frac{\lambda^{[f3]}\lambda^{[f1]}}{m_L^2} < 8\times10^{-0}$	$\frac{\lambda^{f3}\lambda^{f1}}{m_L^2} < 4\times10^{-0}$	$\frac{\lambda^{f3}\lambda^{f1}}{m_L^2} < 4\times10^{-0}$	$\frac{\lambda^{3f}\lambda^{f1}}{m_L^2} < 4\times10^{-0}$	$\frac{\lambda^{3f}\lambda^{f1}}{m_L^2} < 8\times10^{-0}$
$\tau \to \mu\gamma$	$\frac{\lambda^{f3}\lambda^{f2}}{m_L^2} < 7\times10^{-0}$	$\frac{\lambda^{[f3]}\lambda^{[f2]}}{m_L^2} < 1\times10^{+1}$	$\frac{\lambda^{f3}\lambda^{f2}}{m_L^2} < 7\times10^{-0}$	$\frac{\lambda^{f3}\lambda^{f2}}{m_L^2} < 7\times10^{-0}$	$\frac{\lambda^{f3}\lambda^{f2}}{m_L^2} < 7\times10^{-0}$	$\frac{\lambda^{f3}\lambda^{f2}}{m_L^2} < 1\times10^{+1}$
$(\bar{e}e)(\bar{e}e)$	$\frac{\lambda^{11}\lambda^{11}}{m_L^2} < 2\times10^{-0}$		$\frac{\lambda^{11}\lambda^{11}}{m_L^2} < 7\times10^{-1}$		$\frac{\lambda^{11}\lambda^{11}}{m_L^2} < 8\times10^{-1}$	
$(\bar{e}e)(\bar{\mu}\mu)$	$\frac{\lambda^{12}\lambda^{12}}{m_L^2} < 6\times10^{-1}$		$\frac{\lambda^{12}\lambda^{12}}{m_L^2} < 7\times10^{-1}$		$\frac{\lambda^{12}\lambda^{12}}{m_L^2} < 3\times10^{-1}$	
$(\bar{e}e)(\bar{\tau}\tau)$	$\frac{\lambda^{13}\lambda^{13}}{m_L^2} < 3\times10^{-0}$		$\frac{\lambda^{13}\lambda^{13}}{m_L^2} < 7\times10^{-1}$		$\frac{\lambda^{13}\lambda^{13}}{m_L^2} < 1\times10^{-0}$	
$\nu_\mu \to \nu_e, \nu_\tau$				$\frac{\lambda^{11}\lambda^{f2}}{m_L^2} < 1\times10^{-0}$		$\frac{\lambda^{11}\lambda^{f2}}{m_L^2} < 3\times10^{-1}$
		$\frac{\lambda^{[13]}\lambda^{[f2]}}{m_L^2} < 9\times10^{-1}$		$\frac{\lambda^{13}\lambda^{f2}}{m_L^2} < 2\times10^{-0}$		$\frac{\lambda^{13}\lambda^{f2}}{m_L^2} < 9\times10^{-1}$
$\nu_e e \to \nu_e e$					$\frac{\lambda^{11}\lambda^{11}}{m_L^2} < 7\times10^{-0}$	$\frac{\lambda^{11}\lambda^{11}}{m_L^2} < 1\times10^{-0}$

Table 5. Best bounds on λ/m_L for each bilepton, assuming flavour diagonal couplings (4). Note that these are bounds on λ, not λ^2. The processes from which the bounds originate are listed in the third column

$\tilde{L}_1^{--}$	$\frac{\lambda}{m_L} < .5$ TeV^{-1}	$M - \bar{M}$
$L_{2\mu}^{--}$	$\frac{\lambda}{m_L} < .6$ TeV^{-1}	$M - \bar{M}$
$L_{2\mu}^{-}$	$\frac{\lambda}{m_L} < 1$ TeV^{-1}	$\mu_R \to e\nu\nu$
L_3^{--}	$\frac{\lambda}{m_L} < .3$ TeV^{-1}	$M - \bar{M}$
L_3^{-}	$\frac{\lambda}{m_L} < .5$ TeV^{-1}	$\nu_\mu \to \nu_e$

Table 6. Best bounds on λ/m_L for each bilepton, assuming flavour democracy (5). Note that these are bounds on λ, not λ^2. The processes from which the bounds originate are listed in the third column

$\tilde{L}_1^{--}$	$\frac{\lambda}{m_L} < 7 \times 10^{-3}$ TeV^{-1}	$\mu \to 3e$
L_1^{-}	$\frac{\lambda}{m_L} < 6 \times 10^{-2}$ TeV^{-1}	$\mu \to e\gamma$
$L_{2\mu}^{--}$	$\frac{\lambda}{m_L} < 4 \times 10^{-3}$ TeV^{-1}	$\mu \to 3e$
$L_{2\mu}^{-}$	$\frac{\lambda}{m_L} < 3 \times 10^{-2}$ TeV^{-1}	$\mu \to e\gamma$
L_3^{--}	$\frac{\lambda}{m_L} < 4 \times 10^{-3}$ TeV^{-1}	$\mu \to 3e$
L_3^{-}	$\frac{\lambda}{m_L} < 2 \times 10^{-2}$ TeV^{-1}	$\mu \to e\gamma$

pair-production mechanism in hadron collisions may become a possible source of bileptons at LHC energies [35]. Of course, even though by definition bileptons do not couple to quarks, they may also carry a colour charge. In this case hadron colliders may become a major source of bileptons, but we ignore this exotic possibility here.

The present most stringent bounds on bilepton masses originate from their non-observation in the Z^0 decays

$$Z^0 \;\to\; L^0 L^0,\; L^+ L^-,\; L^{++} L^{--} \tag{70}$$

where L represents a generic scalar or vector bilepton. As we shall see, this constrains the bilepton masses to lie above 38 GeV. The advantage of these bounds is that they are firm and do not depend on any unknown lepton-bilepton coupling.

Serious improvements on the present bilepton bounds are expected from experiments at a future linear collider, with a typical energy in the TeV range. A major asset of such a machine is its versatility, as it can be operated in the four e^+e^-, e^-e^-, $e^-\gamma$ and $\gamma\gamma$ modes, with highly polarized electron and photon beams. The typical linear collider designs aim at an integrated yearly e^+e^- luminosity scaling with the squared center of mass energy s like

$$\mathcal{L}_{e^+e^-}\ [\text{fb}^{-1}] \;= 80s\ [\text{TeV}^2] \qquad \text{or} \qquad \mathcal{L}_{e^+e^-} \simeq 3\times 10^7 s\ . \tag{71}$$

We shall present our results in such a way that departures from this working assumption are trivial to implement.

For the doubly-charged bileptons $\tilde{L}_1^{--}$, $L_{2\mu}^{--}$ and L_3^{--}, indirect searches are possible in e^+e^- and e^-e^- scattering [79] through the reactions:

$$e^+e^- \;\to\; e^+e^- \tag{72}$$
$$e^+e^- \;\to\; \ell^+\ell^- \tag{73}$$
$$e^+e^- \;\to\; e^+\ell^- \tag{74}$$
$$e^-e^- \;\to\; e^-e^- \tag{75}$$
$$e^-e^- \;\to\; \ell^-\ell^- \tag{76}$$
$$e^-e^- \;\to\; e^-\ell^-\ , \tag{77}$$

where $\ell = \mu, \tau$. The analysis of these processes may significantly improve the excluded ratios λ/m_L obtained by low-energy data, and provide additional information on the structure of the coupling constants matrix.

In the event an anomaly is observed, though, it may as well be due to other "new physics" effects. In this case, such indirect evidence is no substitute for direct searches.

The lowest order reactions producing bileptons are the following:

$$e^-e^- \;\to\; L^{--} \tag{78}$$
$$e^+e^- \;\to\; L^+\, L^- \tag{79}$$
$$e^+e^- \;\to\; L^{++}\, L^{--} \tag{80}$$
$$e^-\gamma \;\to\; \bar{\nu}\, L^- \tag{81}$$
$$e^-\gamma \;\to\; e^+\, L^{--} \tag{82}$$
$$\gamma\gamma \;\to\; L^+\, L^- \tag{83}$$
$$\gamma\gamma \;\to\; L^{++}\, L^{--}\ . \tag{84}$$

If the center of mass energy reaches the mass of a doubly-charged bilepton $\tilde{L}_1^{--}$, $L_{2\mu}^{--}$ and L_3^{--}, a clearly outstanding resonance is expected from the reactions (78). This e^-e^- annihilation process obviously dwarfs the other reactions (80,82,84), which therefore need not be considered.

Similarly, the singly-charged bileptons L_1^- and L_3^-, are obtained best in the $e^-\gamma$ linear collider operating mode via the reactions (81). Indeed, this way the bileptons need not be pair produced as in reactions (79,83), and can be observed with lower center of mass energies.

In the event the lepton-bilepton couplings are small, though, it may be difficult to resolve the bileptonic signal in the reactions (81). In this case the reactions (79,83) offer an interesting alternative, since they can proceed via the photon or Z^0 couplings to bileptons, which always remain sizable.

As for low-energy experiments, the most problematic bilepton is the neutral L_3^0, which does not couple to charged leptons and will hence be more difficult to produce and to detect in standard high-energy experiments. The only bounds which we can think of, stem from the

Table 7. Best bounds on λ^i/m_L for each bilepton, assuming flavour infiltration (7). The superscript "i" is a generation index. Note that these are bounds on λ, not λ^2. The processes from which the bounds originate are listed below each bound

$\tilde{L}_1^{--}$	$\frac{\lambda^1}{m_L} < .1$ TeV^{-1}	$\frac{\lambda^2}{m_L} < .6$ TeV^{-1}	$\frac{\lambda^3}{m_L} < 11$ TeV^{-1}
	$\mu \to 3e$	$\mu \to e\gamma$	$\tau \to \mu\gamma$
L_1^-	$\frac{\lambda^1}{m_L} < 50$ TeV^{-1}	$\frac{\lambda^2}{m_L} < 8$ TeV^{-1}	$\frac{\lambda^3}{m_L} < 8$ TeV^{-1}
	G_μ	G_τ	G_τ
$L_{2\mu}^{--}$	$\frac{\lambda^1}{m_L} < .06$ TeV^{-1}	$\frac{\lambda^2}{m_L} < .6$ TeV^{-1}	$\frac{\lambda^3}{m_L} < 11$ TeV^{-1}
	$\mu \to 3e$	$\mu \to e\gamma$	$\tau \to \mu\gamma$
$L_{2\mu}^-$	$\frac{\lambda^1}{m_L} < .6$ TeV^{-1}	$\frac{\lambda^2}{m_L} < .6$ TeV^{-1}	$\frac{\lambda^3}{m_L} < 11$ TeV^{-1}
	$\mu \to e\gamma$	$\mu \to e\gamma$	$\tau \to \mu\gamma$
L_3^{--}	$\frac{\lambda^1}{m_L} < .06$ TeV^{-1}	$\frac{\lambda^2}{m_L} < .5$ TeV^{-1}	$\frac{\lambda^3}{m_L} < 11$ TeV^{-1}
	$\mu \to 3e$	$\mu \to e\gamma$	$\tau \to \mu\gamma$
L_3^-	$\frac{\lambda^1}{m_L} < .3$ TeV^{-1}	$\frac{\lambda^2}{m_L} < .3$ TeV^{-1}	$\frac{\lambda^3}{m_L} < 7$ TeV^{-1}
	$\mu \to e\gamma$	$\mu \to e\gamma$	$\tau \to \mu\gamma$

invisible Z^0 width. If someday a Z' resonance is reached, a similar analysis will of course further constrain the L_3^0 mass.

4.1 Z^0 decay

The tree-level Z^0 decay widths (70) into a pair of scalar [20,35,36] or vector bileptons are given by:

$$\Gamma(J=0) = \frac{\alpha Q_Z^2}{12} m_Z \beta^3 \tag{85}$$

$$\Gamma(J=1) = \frac{\alpha Q_Z^2}{12} m_Z \beta^3 \frac{1}{1-\beta^2} \times \left[7 - 12\kappa + 4\kappa^2 - 3\beta^2 + 4\kappa^2 \frac{1}{1-\beta^2}\right] , \tag{86}$$

where

$$\beta = \sqrt{1 - \frac{4m_L^2}{m_Z^2}} \tag{87}$$

and κ_Z is the weak anomalous coupling (9).

Since the four LEP experiments report no serious deviation of the Z^0 width measurement with its standard model prediction, the bilepton contributions (85,86) to the charged lepton or invisible widths may not exceed the experimental error, which amount to 0.27 MeV and 4.2 MeV respectively [51].

We do not know *a priori* the value of the anomalous weak coupling κ_Z in (86). The most conservative LEP bounds on vector bileptons are given by the value of κ_Z which minimizes the width

$$\kappa_{\min} = -\frac{3}{2}\frac{1-\beta^2}{2-\beta^2} . \tag{88}$$

The corresponding vector width is then given by

$$\Gamma_{\min}(J=1) = \frac{\alpha Q_Z^2}{12} m_Z \frac{\beta^3(5 - 4\beta^2 + 3\beta^4)}{(1-\beta^2)(2-\beta^2)} . \tag{89}$$

We plot $\Gamma_{\min}$ in Fig. 7 as a function of the bilepton mass. The least constrained bilepton turns out to be $L_{2\mu}^{--}$, whose coupling to the Z^0 vanishes in the limit $\sin^2\theta_w = 1/4$. Any mass above *ca* 38 GeV is allowed. The other bileptons L_1^-, L_3^-, L_3^0 must lie above 44 GeV and $\tilde{L}_1^{--}$, L_3^{--}, $L_{2\mu}^-$ above 45 GeV.

These results are confirmed by dedicated searches for doubly-charged Higgs bosons [39,41]. Of course, more specific dedicated searches for four-lepton events or highly ionizing tracks (in the event the bilepton couples so weakly to leptons that it decays outside the detector) may improve these bounds, which anyway correspond to the worst case scenario where κ_Z is tuned as in (88).

Virtual bileptons may also enhance the four-lepton events rates, if their couplings to leptons are large. However, the bounds obtainable this way cannot compete with those from low-energy data [43].

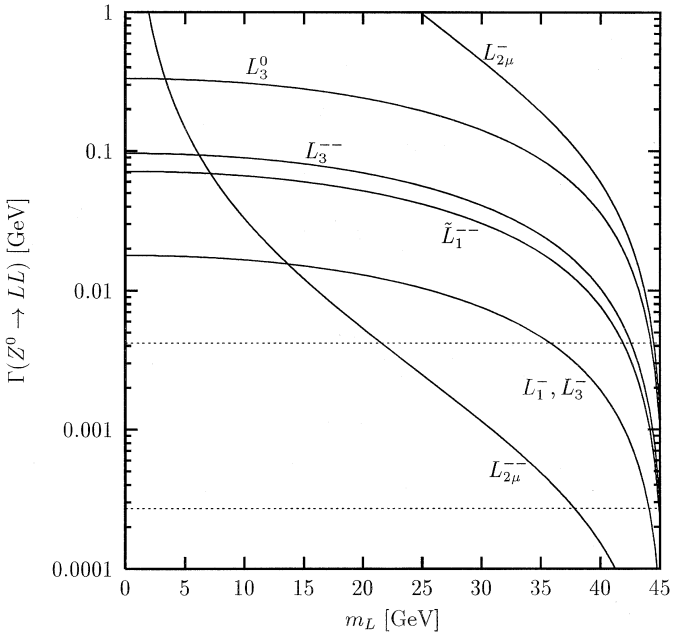

Fig. 7. Partial decay widths of the Z^0 into pairs of bileptons as a function of the bilepton mass. The *lower dotted line* shows the largest partial width consistent with data for the charged bileptons, whereas the *upper dotted line* represents the same limit for the neutral bilepton L_3^0

4.2 Indirect signals

The doubly-charged bileptons $\tilde{L}_1^{--}$, $L_{2\mu}^{--}$ and L_3^{--} contribute to both Bhabha and Møller scattering [79], even if they are too heavy to be directly produced at the given collider energy. They can therefore be detected via deviations from the standard model expectations for the total cross sections and angular correlations. In the presence of off-diagonal flavour couplings, they may even produce final states which are not expected in the realm of the standard model.

These processes have been considered previously for the doubly-charged scalar bileptons in the context of triplet Higgs models [8,20,36], as well as for doubly-charged gauge bileptons [29,80]. Contrary to the claim of [8], we do not find any chiral suppression in the scalar sector.

4.2.1 e^+e^- scattering

Doubly-charged bileptons contribute to Bhabha scattering (72) via their u-channel exchange as depicted in Fig. 8. The corresponding polarized differential cross sections in the case of the exchange of the scalar L_1^{--} are given by

$$\frac{d\sigma(e^+e^- \to e^+e^-, \tilde{L}_1^{--})}{dt} = \frac{4\pi\alpha^2}{s^2} \times \left\{ [RR] \left[\left(\sum_i R_i^2 \left(\frac{u}{s-m_i^2} + \frac{u}{t-m_i^2} \right) \right)^2 + 2\frac{\lambda^2}{e^2} \frac{u}{u-m_L^2} \right)^2 + \left(\sum_i L_i R_i \frac{t}{s-m_i^2} \right)^2 \right] + [LL] \left[\left(\sum_i L_i^2 \left(\frac{u}{s-m_i^2} + \frac{u}{t-m_i^2} \right) \right)^2 + \left(\sum_i L_i R_i \frac{t}{s-m_i^2} \right)^2 \right] + [LR] \left(\sum_i L_i R_i \frac{s}{t-m_i^2} \right)^2 \right\} , \quad (90)$$

where e is the charge of the electron, $\alpha = e^2/4\pi$, $\lambda = \lambda_{ee}$ is the generic diagonal coupling of the bilepton and s, t and u are the Mandelstam variables. The dependence on the polarizations of the positron and electron beams $P_\pm$ is contained in the factors

$$[RR] = \frac{1 + P_+ + P_- + P_+P_-}{4} \quad (91)$$
$$[LL] = \frac{1 - P_+ - P_- + P_+P_-}{4}$$
$$[LR] = \frac{1 - P_+P_-}{2} .$$

The summation runs over $i = \gamma, Z^0$ and the standard model couplings of the photon and Z^0 boson to left- and right-handed leptons are given by

$$\begin{cases} R_\gamma = 1 \\ L_\gamma = 1 \end{cases} \qquad \begin{cases} R_{Z^0} = -\dfrac{\sin\theta_w}{\cos\theta_w} \\ L_{Z^0} = \dfrac{1 - 2\sin^2\theta_w}{2\sin\theta_w\cos\theta_w} \end{cases} . \quad (92)$$

Similarly, the contribution due to L_3^{--} is given by the simple replacements

$$\frac{d\sigma(L_3^{--})}{dt} = \frac{d\sigma(\tilde{L}_1^{--})}{dt} \left(\lambda \to \sqrt{2}\lambda, [LL] \leftrightarrow [RR] \right) . \quad (93)$$

The cross section for e^+e^- annihilation into a pair of other leptons ℓ (73) is easily obtained from (90) by suppressing the γ, Z^0 t-channel exchanges and replacing the diagonal coupling constants matrix element λ by the off-diagonals $\lambda_{e\ell}$ and $\lambda_{\ell e}$.

Similarly, if there are simultaneously diagonal and off-diagonal bilepton couplings, the cross section for reaction (74) is obtained by keeping only the non-standard model u-channel contributions and replacing λ^2 by $\lambda_{ee}\lambda_{e\ell}$ and $\lambda_{ee}\lambda_{\ell e}$.

For the exchange of the vector bilepton, we find the differential cross sections

$$\frac{d\sigma(e^+e^- \to e^+e^-, L_{2\mu}^{--})}{dt} = \frac{4\pi\alpha^2}{s^2} \quad (94)$$
$$\left\{ [RR] \left[\left(\sum_i R_i^2 \left(\frac{u}{s-m_i^2} + \frac{u}{t-m_i^2} \right) \right)^2 \right.$$

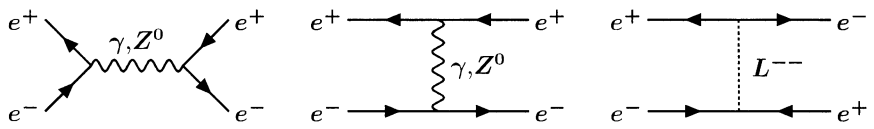

Fig. 8. Lowest order Feynman diagrams contributing to $e^+e^- \to e^+e^-$ scattering. The exchanged doubly-charged bilepton L^{--} in the third diagram, can be either the scalars $\tilde{L}_1^{--}, L_3^{--}$ or the vector $L_{2\mu}^{--}$

$$
\begin{aligned}
&+\left(\sum_i L_i R_i \frac{t}{s-m_i^2} - \frac{\lambda^2}{e^2}\frac{t}{u-m_L^2}\right)^2 \\
&+\left(\frac{\lambda^2}{e^2}\frac{t}{u-m_L^2}\right)^2\Bigg] \\
&+[LL]\left[\left(\sum_i L_i^2\left(\frac{u}{s-m_i^2}+\frac{u}{t-m_i^2}\right)\right)^2\right. \\
&+\left(\sum_i L_i R_i \frac{t}{s-m_i^2} - \frac{\lambda^2}{e^2}\frac{t}{u-m_L^2}\right)^2 \\
&+\left(\frac{\lambda^2}{e^2}\frac{t}{u-m_L^2}\right)^2\Bigg] \\
&+[LR]\left(\sum_i L_i R_i \frac{s}{t-m_i^2} - \frac{\lambda^2}{e^2}\frac{s}{u-m_L^2}\right)^2\Bigg\} \ .
\end{aligned}
$$

The unpolarized ($P_+ = P_- = 0$) differential cross section (94) coincides with the one given in [29] but disagrees with [80].

The cross section for reaction (73) is obtained from (94) by suppressing the γ, Z^0 t-channel exchanges as well as the $[LR]$ term and by replacing the diagonal coupling constants matrix element λ by the off-diagonals $\lambda_{e\ell}$ in the $[RR]$ term and $\lambda_{\ell e}$ in the $[LL]$ term.

Similarly, the cross section for reaction (74) is obtained by droping all the standard model γ and Z^0 terms, by replacing λ^2 by $\lambda_{ee}\lambda_{e\ell}$ in the $[RR]$ term and $\lambda_{ee}\lambda_{\ell e}$ in the $[LL]$ term, and by replacing λ^4 by $\lambda_{ee}^2\left(\lambda_{e\ell}+\lambda_{\ell e}\right)/2$ in the $[LR]$ term.

4.2.2 e^-e^- scattering

As depicted in Fig. 9, doubly-charged bileptons contribute to Møller scattering (75) via their s-channel exchange [79]. The corresponding polarized differential cross sections can of course be obtained from those in Bhabha scattering by crossing symmetry. In the case of the scalar exchange they are given by

$$
\begin{aligned}
\frac{d\sigma(e^-e^- \to e^-e^-, \tilde{L}_1^{--})}{dt} &= \frac{2\pi\alpha^2}{s^2} \\
\Bigg\{[RR]&\left[\sum_i R_i^2\left(\frac{s}{t-m_i^2}+\frac{s}{u-m_i^2}\right)\right. \\
&\left.+2\frac{\lambda^2}{e^2}\frac{s}{s-m_L^2}\right]^2
\end{aligned}
\tag{95}
$$

$$
\begin{aligned}
&+[LL]\left[\sum_i L_i^2\left(\frac{s}{t-m_i^2}+\frac{s}{u-m_i^2}\right)\right]^2 \\
&+[LR]\left[\left(\sum_i L_i R_i \frac{t}{u-m_i^2}\right)^2\right. \\
&\left.\left.+\left(\sum_i L_i R_i \frac{u}{t-m_i^2}\right)^2\right]\right\} \ ,
\end{aligned}
$$

where we have used the same notations as in the previous section.

Again, as in the e^+e^- case, the cross sections for the L_3^{--} exchange are related to (95) by the substitutions (93).

Similarly, for the exchange of the vector bilepton, we find the differential cross sections

$$
\begin{aligned}
\frac{d\sigma(e^-e^- \to e^-e^-, L_{2\mu}^{--})}{dt} &= \frac{2\pi\alpha^2}{s^2} \\
\Bigg\{[RR]&\left[\sum_i R_i^2\left(\frac{s}{t-m_i^2}+\frac{s}{u-m_i^2}\right)\right]^2 \\
&+[LL]\left[\sum_i L_i^2\left(\frac{s}{t-m_i^2}+\frac{s}{u-m_i^2}\right)\right]^2 \\
&+[LR]\left[\left(\sum_i L_i R_i \frac{t}{u-m_i^2} - \frac{\lambda^2}{e^2}\frac{t}{s-m_L^2}\right)^2\right. \\
&\left.\left.+\left(\sum_i L_i R_i \frac{u}{t-m_i^2} - \frac{\lambda^2}{e^2}\frac{u}{s-m_L^2}\right)^2\right]\right\} \ .
\end{aligned}
\tag{96}
$$

The cross sections for the reactions (76,77), which produce leptons ℓ other than electrons are easily obtained from (95) and (96) by keeping only the non-standard model s-channel contributions and replacing λ^2 by either $\lambda_{ee}\lambda_{\ell\ell}$ or $\lambda_{ee}\lambda_{e\ell}$.

4.2.3 Discovery limits

The Bhabha scattering data gathered below the Z^0 peak has allowed to constrain the scalar [20,36] and vector [29] bilepton masses and coupling by

$$
\frac{\tilde{\lambda}_1^{ee}}{m_L} \lesssim 4.4 \qquad \frac{\lambda_2^{ee}}{m_L} \lesssim 2.1 \qquad \frac{\lambda_3^{ee}}{m_L} \lesssim 3.1 \tag{97}
$$

at the 95 % confidence level. A similar analysis of the LEP data above the Z could improve these bounds, with sufficient luminosity.

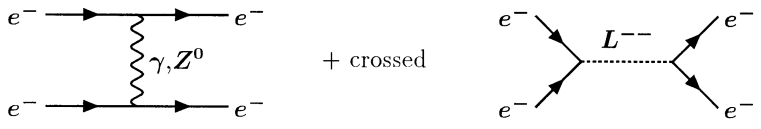

Fig. 9. Lowest order Feynman diagrams contributing to $e^-e^- \to e^-e^-$ scattering. The exchanged doubly-charged bilepton L^{--} in the third diagram, can be either the scalars $\tilde{L}_1^{--}, L_3^{--}$ or the vector $L_{2\mu}^{--}$

To gauge the discovery potential of the reactions (72–77), it is instructive to work in the limits

$$|P| = 1 \qquad m_Z^2 \ll s \ll m_L^2 \qquad \sin^2\theta_w = \frac{1}{4}\ , \tag{98}$$

where the propagators and the standard model γ, Z^0 couplings (92) simplify drastically.

The reactions (74,76,77) cannot take place in the realm of the standard model. Given the spectacular nature of lepton flavour violation, we estimate that five events should suffice to establish a discovery. We therefore need an average number of 9.15 Poisson distributed events such that *at least* 5 events are observed with 95% probability.

The average number of events is given by

$$N = \mathcal{L}\int dt \frac{d\sigma}{dt}\ , \tag{99}$$

where $\mathcal{L}$ is the integrated luminosity. Because there will be some amount of anti-pinch at the interaction point for the e^-e^- mode, we assume it can only achieve half the luminosity of the e^+e^- mode [83]:

$$\mathcal{L}_{e^-e^-} = \mathcal{L}_{e^+e^-}/2\ , \tag{100}$$

where the e^+e^- luminosity follows the energy scaling law (71).

For the reactions (72,73,75), which do take place whether there are bileptons or not, we compute the Cramér-Rao limit (*cf.* Appendix B)

$$\chi^2_\infty = \mathcal{L}\int dt \frac{\left(\dfrac{d\sigma(\lambda)}{dt} - \dfrac{d\sigma(\lambda=0)}{dt}\right)^2}{\dfrac{d\sigma(\lambda=0)}{dt}}\ . \tag{101}$$

Setting the value of the estimator χ^2_∞ equal to 3.84, we obtain the 95% confidence bounds on the parameter λ.

The particularly clean environment of the e^+e^- and above all e^-e^- collisions, largely justifies here the neglect of systematic errors.

It is straightforward to obtain the following lower bounds on the observable values of the ratios λ/m_L:

reaction	polarization	bilepton	bound
$e^+e^- \to e^+e^-$	$P_- = P_+ = +1$	$\tilde{L}_1^{--}$	$\frac{\lambda_{ee}^2}{m_L^2} \geq .23\sqrt{\frac{16\pi\chi^2_\infty}{s\mathcal{L}_{e^+e^-}}}$
	$P_- = P_+ = -1$	L_3^{--}	$\frac{\lambda_{ee}^2}{m_L^2} \geq .11\sqrt{\frac{16\pi\chi^2_\infty}{s\mathcal{L}_{e^+e^-}}}$
	$P_- = P_+ = \pm 1$	$L_{2\mu}^{--}$	$\frac{\lambda_{ee}^2}{m_L^2} \geq .49\sqrt{\frac{16\pi\chi^2_\infty}{s\mathcal{L}_{e^+e^-}}}$
	$P_- = -P_+ = \pm 1$	$L_{2\mu}^{--}$	$\frac{\lambda_{ee}^2}{m_L^2} \geq .25\sqrt{\frac{16\pi\chi^2_\infty}{s\mathcal{L}_{e^+e^-}}}$
$e^+e^- \to \ell^+\ell^-$	$P_- = P_+ = +1$	$\tilde{L}_1^{--}$	$\frac{\lambda_{e\ell}^2}{m_L^2} \geq .22\sqrt{\frac{16\pi\chi^2_\infty}{s\mathcal{L}_{e^+e^-}}}$
	$P_- = P_+ = -1$	L_3^{--}	$\frac{\lambda_{e\ell}^2}{m_L^2} \geq .11\sqrt{\frac{16\pi\chi^2_\infty}{s\mathcal{L}_{e^+e^-}}}$
	$P_- = P_+ = \pm 1$	$L_{2\mu}^{--}$	$\frac{\lambda_{e\ell}^2}{m_L^2} \geq .53\sqrt{\frac{16\pi\chi^2_\infty}{s\mathcal{L}_{e^+e^-}}}$
	$P_- = -P_+ = \pm 1$	$L_{2\mu}^{--}$	$\frac{\lambda_{e\ell}^2}{m_L^2} \geq .50\sqrt{\frac{16\pi N}{s\mathcal{L}_{e^+e^-}}}$
$e^+e^- \to e^+\ell^-$	$P_- = P_+ = +1$	$\tilde{L}_1^{--}$	$\frac{\lambda_{ee}}{m_L}\frac{\lambda_{e\ell}}{m_L} \geq .31\sqrt{\frac{16\pi N}{s\mathcal{L}_{e^+e^-}}}$
	$P_- = P_+ = -1$	L_3^{--}	$\frac{\lambda_{ee}}{m_L}\frac{\lambda_{e\ell}}{m_L} \geq .15\sqrt{\frac{16\pi N}{s\mathcal{L}_{e^+e^-}}}$
	$P_- = P_+ = \pm 1$	$L_{2\mu}^{--}$	$\frac{\lambda_{ee}}{m_L}\frac{\lambda_{e\ell}}{m_L} \geq .61\sqrt{\frac{16\pi N}{s\mathcal{L}_{e^+e^-}}}$
	$P_- = -P_+ = \pm 1$	$L_{2\mu}^{--}$	$\frac{\lambda_{ee}}{m_L}\frac{\lambda_{e\ell}}{m_L} \geq .50\sqrt{\frac{16\pi N}{s\mathcal{L}_{e^+e^-}}}$
$e^-e^- \to e^-e^-$	$P_1 = P_2 = +1$	$\tilde{L}_1^{--}$	$\frac{\lambda_{ee}^2}{m_L^2} \geq .18\sqrt{\frac{16\pi\chi^2_\infty}{s\mathcal{L}_{e^+e^-}}}$
	$P_1 = P_2 = -1$	L_3^{--}	$\frac{\lambda_{ee}^2}{m_L^2} \geq .09\sqrt{\frac{16\pi\chi^2_\infty}{s\mathcal{L}_{e^+e^-}}}$
	$P_1 = -P_2 = \pm 1$	$L_{2\mu}^{--}$	$\frac{\lambda_{ee}^2}{m_L^2} \geq .44\sqrt{\frac{16\pi\chi^2_\infty}{s\mathcal{L}_{e^+e^-}}}$
$e^-e^- \to \ell^-\ell^-$	$P_1 = P_2 = +1$	$\tilde{L}_1^{--}$	$\frac{\lambda_{ee}}{m_L}\frac{\lambda_{\ell\ell}}{m_L} \geq .35\sqrt{\frac{16\pi N}{s\mathcal{L}_{e^+e^-}}}$
	$P_1 = P_2 = -1$	L_3^{--}	$\frac{\lambda_{ee}}{m_L}\frac{\lambda_{\ell\ell}}{m_L} \geq .18\sqrt{\frac{16\pi N}{s\mathcal{L}_{e^+e^-}}}$
	$P_1 = -P_2 = \pm 1$	$L_{2\mu}^{--}$	$\frac{\lambda_{ee}}{m_L}\frac{\lambda_{\ell\ell}}{m_L} \geq .87\sqrt{\frac{16\pi N}{s\mathcal{L}_{e^+e^-}}}$
$e^-e^- \to e^-\ell^-$	$P_1 = P_2 = +1$	$\tilde{L}_1^{--}$	$\frac{\lambda_{ee}}{m_L}\frac{\lambda_{e\ell}}{m_L} \geq .25\sqrt{\frac{16\pi N}{s\mathcal{L}_{e^+e^-}}}$
	$P_1 = P_2 = -1$	L_3^{--}	$\frac{\lambda_{ee}}{m_L}\frac{\lambda_{e\ell}}{m_L} \geq .13\sqrt{\frac{16\pi N}{s\mathcal{L}_{e^+e^-}}}$
	$P_1 = -P_2 = \pm 1$	$L_{2\mu}^{--}$	$\frac{\lambda_{ee}}{m_L}\frac{\lambda_{e\ell}}{m_L} \geq .61\sqrt{\frac{16\pi N}{s\mathcal{L}_{e^+e^-}}}$

If the positrons cannot be polarized, the e^+e^- bounds are worsened by a factor $\sqrt{2}$.

The bounds at 95% confidence level are obtained by setting $\chi^2_\infty = 3.84$ and $N = 9.15$. Note that the reactions which are allowed or forbidden within the realm of the standard model all yield similar results. Indeed, although the allowed reactions need much more anomalous events to be statistically relevant, this number of anomalous events is very much enhanced by the interferences with the standard model channels.

4.3 Direct signals

If the center of mass energy of the collider is sufficient to produce bileptons, their decay widths becomes an issue of importance. As we ignore self-interactions and assume the scalars do not develop a vacuum expectation value, the bileptons cannot decay weakly into a single or a pair of gauge bosons. Therefore, the leptonic two-body decay modes are dominant. Setting all lepton masses to zero, the scalar bilepton widths are

$$\Gamma = A\frac{m_L}{8\pi}\sum_{ij}\lambda_{ij}^2 \ , \tag{102}$$

where $A = 1/2, 1, 1/3, 2$ for $L_1,\ \tilde{L}_1,\ L_{2\mu},\ L_3$ respectively and the sum runs over all elements of the coupling constants matrix ($i,j = e,\mu,\tau$). The doubly-charged vector width agrees with the width computed in [29] and disagrees with [80], while the doubly-charged scalar widths agree with [20,35,36] and disagree with [8].

If the indirect searches from experiments below the real production threshold have been unsuccessful, the leptonic couplings are unlikely to exceed 0.2 and one can safely state that the total bilepton width Γ_L is narrow:

$$\Gamma_L \leq 10^{-2} m_L \ . \tag{103}$$

Of course, this argumentation does not directly apply to the neutral and singly-charged bileptons and may break down for some perverse choices of coupling matrices. We ignore this possibility here.

4.3.1 e^-e^- scattering

As depicted in Fig. 10, a doubly-charged bilepton can be produced in e^-e^- collisions (78) and subsequently decay into a pair of leptons [79]. The corresponding polarized cross sections for the production and decay of scalars or vectors is obtained by replacing the s-channel propagator in (95,96) by a Breit-Wigner resonance with the correct width (102). On the resonance $s = m_L^2$, we may ignore other possible channels and find the cross sections

$$\begin{aligned}&\sigma(e^-e^- \to \ell^-\ell'^-, J=0)\\ &= \frac{1+P_1P_2}{2}\frac{32\pi}{m_L^2}\left(\frac{\lambda_{ee}\lambda\ell\ell'}{\sum_{ij}\lambda_{ij}^2}\right)^2 \end{aligned}\tag{104}$$

$$\begin{aligned}&\sigma(e^-e^- \to \ell^-\ell'^-, J=1)\\ &= \frac{1-P_1P_2}{2}\frac{48\pi}{m_L^2}\left(\frac{\lambda_{ee}\lambda\ell\ell'}{\sum_{ij}\lambda_{ij}^2}\right)^2 \ , \end{aligned}\tag{105}$$

where $\ell\ell' = e,\mu,\tau$. The total number of events expected on any bilepton peak is thus of the order of

$$n = \mathcal{L}\sigma \approx 10^7 \frac{\mathcal{L}[\mathrm{fb}^{-1}]}{m_L^2[\mathrm{TeV}^2]}\left(\frac{\lambda_{ee}\lambda\ell\ell'}{\sum_{ij}\lambda_{ij}^2}\right)^2 \ , \tag{106}$$

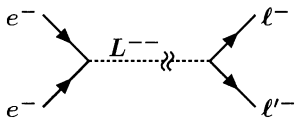

Fig. 10. Lowest order Feynman diagram for the production of a doubly-charged bilepton L^{--} in e^-e^- collisions. The produced bilepton can be either a scalar $\tilde{L}_1^{--}, L_3^{--}$ or the vector $L_{2\mu}^{--}$

where the last factor is less or equal to one. In any case, whatever finite value it assumes, a spectacular resonance is thus sure to be observed [29]. Note also how conveniently a beam polarization flip can discriminate between scalar and vector bileptons.

If the leptonic couplings are so small, that the bilepton width drops far below the beam energy spread, the signal will be attenuated accordingly. Still, the rates remain substantial, even for minute leptonic couplings [82].

This reaction is so spectacular and unavoidable, that we do not need to consider the production of doubly-charged bileptons in the other linear collider modes.

It has also been advocated [88] to study the cross-channel flavour violating reaction $\mu^+e^- \to \mu^-e^+$, if someday a muon and an electron collider can be combined.

4.3.2 $e^-\gamma$ scattering

In principle, doubly-charged bileptons can be produced in $e^-\gamma$ collisions (82) with substantial cross sections [40]. However, these processes cannot compete with the resonant production in e^-e^- collisions (78). A singly-charged bilepton, though, can also be produced in $e^-\gamma$ scattering (81) as depicted in Fig. 11. As these bileptons decay into a lepton and a neutrino, the signal to be tagged is a lepton and missing energy. The analysis is more complex than in e^-e^- scattering, because

- one has to fold the cross sections (107–109) over the photon energy and polarization spectra [84];
- there is no resonance and the signal is hence weak at threshold;
- the standard model backgrounds from W^- or Z^0 production and subsequent leptonic or invisible decays are substantial.

The polarized differential cross sections for the production of scalar, vector or Yang-Mills fields are given by

$$\begin{aligned}\frac{d\sigma(e^-\gamma \to \bar{\nu}L^-)}{dt} &= \frac{2\pi\alpha^2}{s^2}\frac{\lambda^2}{e^2}\frac{1-P_e}{2}\frac{-u}{s(t-m_L^2)^2}\\ &\left[\frac{1-P_\gamma}{2}t^2 + \frac{1+P_\gamma}{2}m_L^4\right]\end{aligned}\tag{107}$$

$$\begin{aligned}&\frac{d\sigma(e^-\gamma \to \bar{\nu}L_\mu^-, \kappa_\gamma = 0)}{dt}\\ &= \frac{2\pi\alpha^2}{s^2}\frac{\lambda^2}{e^2}\frac{1+P_e}{2}\frac{1}{4m_L^2 s(t-m_L^2)^2}\end{aligned}\tag{108}$$

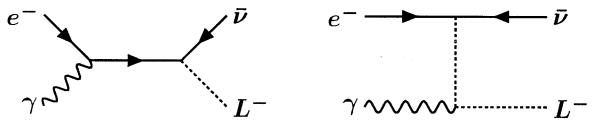

Fig. 11. Lowest order Feynman diagrams for the associate production of a singly-charged bilepton L^- and an anti-neutrino in $e^-\gamma$ collisions. The produced bilepton can be either a scalar L_1^-, L_3^- or the vector $L_{2\mu}^-$. In the case of the L_1^-, the neutrino cannot be of the electron type

$$\left\{\frac{1-P_\gamma}{2}u\left[8um_L^4-tu(s-8m_L^2)-2m_L^2(s-2m_L^2)^2\right]\right.$$
$$\left.-\frac{1+P_\gamma}{2}\left[s^3t+2m_L^2(s-2m_L^2)^2\right]\right\}$$

$$\frac{d\sigma(e^-\gamma\to\bar\nu L_\mu^-,\kappa_\gamma=1)}{dt}$$
$$=\frac{2\pi\alpha^2}{s^2}\frac{\lambda^2}{e^2}\frac{1+P_e}{2}\frac{-2u}{s(t-m_L^2)^2} \qquad (109)$$
$$\left[\frac{1-P_\gamma}{2}(s-m_L^2)^2+\frac{1+P_\gamma}{2}(u-m_L^2)^2\right] .$$

For completeness, we also mention the integrated cross sections for both the singly- and doubly-charged bileptons and for any value of the electric anomalous coupling κ_γ. Defining

$$x=\frac{m_L^2}{s} , \qquad (110)$$

they are given by

$$\sigma(J=0)=\frac{\pi\alpha^2}{2s}\frac{\lambda^2}{e^2}\frac{1\pm P_e}{2}\times \qquad (111)$$
$$\left\{\left(-(3+4Q)+\left(7+8Q+8Q^2\right)x\right)\quad(1-x)\right.$$
$$+4Q\left(Q-(2+Q)x\right)\quad x\ln x$$
$$-2(1+Q)^2\left(1-2x+2x^2\right)\quad\ln\frac{m_\ell^2/s}{(1-x)^2}$$
$$\pm P_\gamma\left[\left(-\left(7+12Q+4Q^2\right)+3x\right)\quad(1-x)\right.$$
$$+4Q^2\quad x\ln x$$
$$\left.\left.-2(1+Q)^2(1-2x)\ln\frac{m_\ell^2/s}{(1-x)^2}\right]\right\}$$

$$\sigma(J=1)=\frac{\pi\alpha^2}{8m^2}\frac{\lambda^2}{e^2}\frac{1\pm P_e}{2}\times \qquad (112)$$
$$\left\{\left(\left(1+30\kappa+\kappa^2\right)Q^2+\left(8-16(1+\kappa)Q-(1-\kappa)^2Q^2\right)x\right.$$
$$\left.+8\left(7+8Q+8Q^2\right)x^2\right)\quad(1-x)$$
$$-4Q\left((1-\kappa)^2Q+(8(1+\kappa)+(1-\kappa)(3+\kappa)Q\right)x$$
$$-8Qx^2+8(2+Q)x^3\big)\quad\ln x$$
$$-16(1+Q)^2\left(1-2x+2x^2\right)\quad x\ln\frac{m_\ell^2/s}{(1-x)^2}$$
$$\pm P_\gamma\left[\left(-3(1-\kappa)^2Q^2+(40+16(3-\kappa)Q\right.\right.$$
$$\left.+(63+34\kappa-\kappa^2)Q^2\right)x+24x^2\big)\quad(1-x)$$
$$-4Q\left(-(3+6\kappa-\kappa^2)Q+8(3+\kappa+Q)x\right)\quad x\ln x$$
$$\left.\left.+16(1+Q)^2(1-2x)x\ln\frac{m_\ell^2/s}{(1-x)^2}\right]\right\} ,$$

where $\kappa=\kappa_\gamma$ and $m_\ell=m_\mu,m_\tau$ is the mass of the u-channel charged lepton exchanged in the production of a doubly-charged bilepton. The unpolarized expressions for the associated electron production are given in [40].

The Z^0 background is entirely confined in the region of phase space where the energy E_ℓ and polar angle θ_ℓ of the single emerging lepton are contained within:

$$E_\ell>\frac{y_{\min}s-m_Z^2}{\sqrt{s}\left[(1-\cos\theta_\ell)+y_{\min}(1+\cos\theta_\ell)\right]} , \qquad (113)$$

where $y=E_\gamma/E_e$ is the energy fraction of the photons. The exact value of its minimum can be tuned by changing the distance between the conversion and interaction points. In the following we assume $y_{\min}=.5$.

Similarly, most of the W^- events are located in the region of phase space where

$$E_\ell<\frac{m_W^2y\sqrt{s}}{y^2s(1+\cos\theta_\ell)+m_W^2(1-\cos\theta_\ell)} . \qquad (114)$$

Since the vector bilepton $L_{2\mu}^-$ couples to right-handed electrons, polarizing accordingly the electron beam will result into a further suppression of the W^- background. Unfortunately, the scalar bileptons L_1^- and L_3^- will need a left polarized electron beam and will thus have to compete with the large W^- background.

To gauge the discovery potential of $e^-\gamma$ collisions, we have plotted in Fig.12 for the scalar bilepton L_1^- and several collider center of mass energies the $\chi^2_\infty=1$ boundary in the (λ,m_L) plane of the Cramér-Rao limit [87] (*cf.* Appendix B)

$$\chi^2_\infty=\mathcal{L}\int dyP(y)\int d\cos\theta_\ell\frac{\left(\frac{d\sigma(\lambda)}{d\cos\theta_\ell}-\frac{d\sigma(\lambda=0)}{d\cos\theta_\ell}\right)^2}{\frac{d\sigma(\lambda=0)}{d\cos\theta_\ell}} . \qquad (115)$$

The photon energy spectrum $P(y)$ is given in [84] and the electron-photon center of mass energy is $\sqrt{s_{e\gamma}}=\sqrt{ys_{ee}}$. To obtain these results we have included all decay channels of the bileptons and have made the following realistic assumptions:

$$\begin{aligned}&\mathcal{L}_{e^+e^-}=20\text{ fb}^{-1} \qquad (116)\\ &|P_e|=90\%\\ &|P_{\text{laser}}|=100\%\\ &.5\le y=E_\gamma/E_e\le.83\\ &\theta_\ell\ge5^o\\ &E_\ell\ge10\text{ GeV} ,\end{aligned}$$

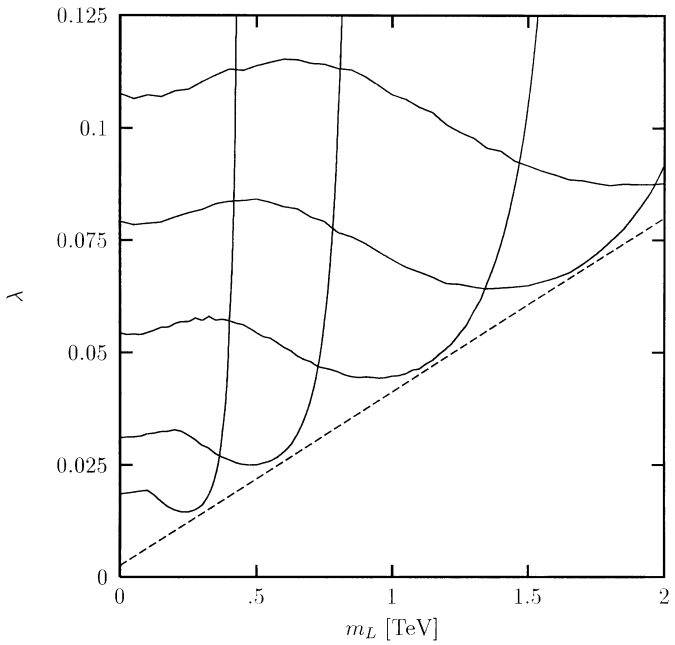

Fig. 12. Smallest observable scalar bilepton L_1^- couplings to leptons at the one standard deviation level. as a function of the bilepton mass in $e^-\gamma$ collisions. The collider's e^+e^- center of mass energies are .5, 1, 2, 3 and TeV from left to right. The other parameters used are given in (116)

where θ_ℓ and E_ℓ are the polar angle and energy of the emerging lepton.

Similar plots are obtained for the vector bileptons. In general, these curves are closely osculated by the relation

$$\sum_\ell \left(\frac{\lambda_1^{e\ell}}{m_L/\mathrm{TeV}}\right)^2 = \sum_\ell \left(\frac{\lambda_3^{e\ell}}{m_L/\mathrm{TeV}}\right)^2 = .15\ \frac{\chi^2_\infty}{\mathcal{L}/\mathrm{fb}^{-1}} \quad (m_L \leq .6\sqrt{s_{ee}}) \tag{117}$$

$$\sum_\ell \left(\frac{\lambda_2^{e\ell}}{m_L/\mathrm{TeV}}\right)^2 = .03\ \frac{\chi^2_\infty}{\mathcal{L}/\mathrm{fb}^{-1}} \quad (m_L \leq .3\sqrt{s_{ee}})\ , \tag{118}$$

where χ^2_∞ is the required number of standard deviations, $\mathcal{L}$ is the integrated luminosity and $\ell = e, \mu, \tau$. These scaling relations provide a convenient means to gauge the bilepton discovery potential of $e^-\gamma$ scattering.

Although the relations (117,118) are only valid for bilepton masses lighter than 60% or 30% of the collider energy, heavier bileptons with stronger couplings can also be probed up to the kinematical limit $m_L \simeq .91\sqrt{s_{ee}}$.

Single bilepton production can also take place via the same submechanism with quasi-real electrons in $\gamma\gamma$ collisions [40] with quasi-real photons in e^+e^- [81,40] or e^-p [42] collisions. As expected, the cross sections are accordingly smaller. It is straightforward to translate the results of [42] for doubly-charged scalar bileptons ligther than

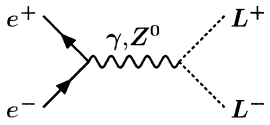

Fig. 13. Lowest order Feynman diagrams contributing to $e^+e^- \to L^+L^-$ scattering, where the final state bileptons can be either the scalars L_1^-, L_3^- or the vector $L_{2\mu}^{--}$

150 GeV, into the approximate HERA exclusion range $\lambda \lesssim 0.65 m_L$ [TeV].

4.3.3 e^+e^- scattering

Doubly-charged bileptons can in principle be pair-produced in e^+e^- scattering (80) [20,35,36,81], but these processes can under no circumstances compete with the resonant production in e^-e^- collisions (78). However, the pair-production of singly-charged bileptons (79) may become interesting if their couplings to leptons turn out to be too small to be observed in $e^-\gamma$ scattering (81). Indeed, as depicted in the Feynman diagram of Fig. 13, bileptons can still be produced thanks to their couplings to the neutral gauge bosons (8,9).

The signal will consist of 2-lepton events with missing energy. The standard model backgrounds from W pair production are substantial, but may be rendered harmless in e^+e^- scattering with right-handed electron beams. As we shall see shortly, this polarization also significantly enhances the signal.

Assuming the bileptons couple so weakly to leptons that their discovery is precluded in $e^-\gamma$ scattering, we can ignore the t-channel lepton exchange in the e^+e^- reaction. Whatever the charge of the produced bileptons, using the definitions (91,92) the integrated scalar [20,35,36,81] and vector e^+e^- cross sections are then

$$\sigma(e^+e^- \to L\bar{L}) = \frac{2\pi\alpha^2}{3s}\Sigma\beta^3 \tag{119}$$

$$\sigma(e^+e^- \to L_\mu\bar{L}_\mu) = \frac{2\pi\alpha^2}{3s}\Sigma\beta^3\frac{1}{1-\beta^2}\Big[7 - 12\kappa + 4\kappa^2 - 3\beta^2 + 4\kappa^2\frac{1}{1-\beta^2}\Big]\ , \tag{120}$$

where

$$\beta = \sqrt{1 - \frac{4m_L^2}{s}} \qquad \kappa = \kappa_\gamma = \kappa_Z \tag{121}$$

and

$$\Sigma = [LL]\left(\sum_{i=\gamma,Z^0}\frac{s}{(s-m_i^2)}Q_iL_i\right)^2 + [RR]\left(\sum_{i=\gamma,Z^0}\frac{s}{(s-m_i^2)}Q_iR_i\right)^2\ . \tag{122}$$

We do not know *a priori* the value of the electroweak anomalous coupling $\kappa = \kappa_\gamma = \kappa_Z$ in (120). The most

conservative bounds to be expected from e^+e^- scattering on vector bileptons are given, like in (88), by the value of κ which minimizes the cross section

$$\kappa_{\min} = -\frac{3}{2}\frac{1-\beta^2}{2-\beta^2} \ . \tag{123}$$

It is only for simplicity, that we assume the electric and weak anomalous coupling to be equal in (121). It must be borne in mind that some unfortunate combinations may suppress the vector cross sections even further. We discard such a possibility here.

In the limits

$$|P_{e^-}| = |P_{e^+}| = 1 \qquad m_Z^2 \ll s \qquad \sin^2\theta_w = \frac{1}{4} \tag{124}$$

the scalar and vector cross sections are then given by

$$\sigma(e_R^+e_R^- \to L^+L^-) = \frac{32\pi\alpha^2}{27s}\beta^3 \tag{125}$$

$$\sigma(e_L^+e_L^- \to L^+L^-) = \frac{1}{4}\sigma(e_R^+e_R^- \to L^+L^-)$$

$$\sigma_{\min}(e_R^+e_R^- \to L_\mu^+L_\mu^-) = \frac{8\pi\alpha^2}{3s}\beta^3\frac{\beta^3(5-4\beta^2+3\beta^4)}{(1-\beta^2)(2-\beta^2)}$$

$$\sigma(e_L^+e_L^- \to L_\mu^+L_\mu^-) = 0 \ . \tag{126}$$

If the positrons cannot be polarized, these cross sections are to be divided by 2.

Assuming the luminosity scaling law (71) and all bilepton decay channels to be observed, we plot in Fig. 14 the number of expected bilepton events in right-polarized e^+e^- collisions as a function of the ratio of bilepton mass to the center of mass energy. Clearly, a significant signal is expected, even close to the kinematical limit.

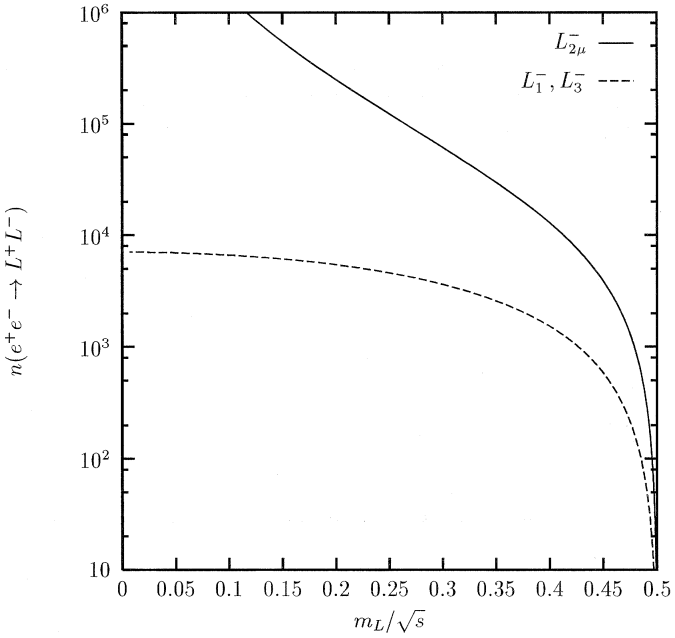

Fig. 14. Mass dependence of the number of pair-produced singly-charged bileptons in e^+e^- annihilations, assuming the luminosity scaling law (71)

4.3.4 $\gamma\gamma$ scattering

In principle bileptons can also be pair-produced in $\gamma\gamma$ collisions (80,84). However, the doubly-charged bileptons will be much better observed in e^-e^- scattering. Similarly, $e^-\gamma$ collisions or e^+e^- annihilations with a right-handed electron beam will offer a better signal to background ratio. Moreover, the $\gamma\gamma$ center of mass energy cannot exceed *ca* 83% of the e^+e^- collider energy. For all these reasons, $\gamma\gamma$ collisions are only of marginal interest for discovering bileptons, and we do not consider these reactions here.

4.4 High-energy summary

The present and prospective high-energy bounds on $L = 2$ bileptons are summarized in Tables 8 and 9. Only the limits from the experiments which provide the best constraints on the bilepton masses and couplings to leptons are listed. All bounds are stated at the 95% confidence level.

The LEP experiments constrain all bileptons to have a mass exceeding at least 44 GeV, except for the doubly-charged vector $L_{2\mu}^{--}$ which couples very weakly to the Z^0 bosons and could still be as light as 38 GeV. These bounds are totally model-independent.

In high-energy Bhabha and Møller scattering virtual doubly-charged bileptons may induce corrections or even lepton flavour violations. The non-observation of such effects at a linear collider of the next generation will allow stringent limits to be set on the ratio of the leptonic coupling to the mass λ/m_L. This will substantially improve the low-energy bounds. Moreover, the discovery prospects are to a much lesser extent dependent on the structure of the flavour coupling matrix.

If the collider center of mass energy reaches the mass of a doubly-charged bilepton, it will show up as a spectacular resonance in e^-e^- scattering. This is therefore the privileged mode for discovering and studying the properties of doubly-charged bileptons.

Singly-charged bileptons can be produced both in e^+e^- and $e^-\gamma$ scattering. Provided the collider energy is sufficient to pair-produce bileptons, the e^+e^- mode can probe bileptons which couple very weakly to leptons and hence provide model-independent mass limits. Heavier bileptons can be searched for in $e^-\gamma$ reactions, if their couplings to leptons are not too weak.

Once bileptons are produced on-shell, the information gathered from their cross sections and their decay modes will unambiguously determine a large portion of the coupling constant matrix.

Unless a Z' resonance is directly accessible, standard high-energy experiments have no prospects for seeing the neutral bilepton L_3^0.

Table 8. Best explorable limits on the coupling to mass ratio of the doubly-charged bileptons in indirect high-energy e^-e^- and e^+e^- searches. These 95% confidence bounds are given for the three flavour coupling models (4–7). We assume unpolarized positron beams and use the luminosities (71,100) for the e^+e^- and e^-e^- mode

	e^-e^-			e^+e^-		
	diagonal	democracy	infiltration	diagonal	democracy	infiltration
$\tilde{L}_1^{--}$	$\frac{\lambda}{m} > \frac{0.02}{\sqrt{s}}$	$\frac{\lambda}{m} > \frac{0.02}{\sqrt{s}}$	$\frac{\lambda^1}{m} > \frac{0.02}{\sqrt{s}}$ $\frac{\lambda^1}{m}\frac{\lambda^2}{m} > \frac{0.001}{s}$ $\frac{\lambda^1}{m}\frac{\lambda^3}{m} > \frac{0.001}{s}$	$\frac{\lambda}{m} > \frac{0.025}{\sqrt{s}}$	$\frac{\lambda}{m} > \frac{0.025}{\sqrt{s}}$	$\frac{\lambda^1}{m} > \frac{0.025}{\sqrt{s}}$ $\frac{\lambda^2}{m} > \frac{5}{\sqrt{s}}$ $\frac{\lambda^3}{m} > \frac{82}{\sqrt{s}}$
$L_{2\mu}^{--}$	$\frac{\lambda}{m} > \frac{0.035}{\sqrt{s}}$	$\frac{\lambda}{m} > \frac{0.035}{\sqrt{s}}$	$\frac{\lambda^1}{m} > \frac{0.035}{\sqrt{s}}$ $\frac{\lambda^1}{m}\frac{\lambda^2}{m} > \frac{0.003}{s}$ $\frac{\lambda^1}{m}\frac{\lambda^3}{m} > \frac{0.003}{s}$	$\frac{\lambda}{m} > \frac{0.025}{\sqrt{s}}$	$\frac{\lambda}{m} > \frac{0.025}{\sqrt{s}}$	$\frac{\lambda^1}{m} > \frac{0.025}{\sqrt{s}}$ $\frac{\lambda^2}{m} > \frac{8}{\sqrt{s}}$ $\frac{\lambda^3}{m} > \frac{128}{\sqrt{s}}$
L_3^{--}	$\frac{\lambda}{m} > \frac{0.015}{\sqrt{s}}$	$\frac{\lambda}{m} > \frac{0.015}{\sqrt{s}}$	$\frac{\lambda^1}{m} > \frac{0.015}{\sqrt{s}}$ $\frac{\lambda^1}{m}\frac{\lambda^2}{m} > \frac{0.0007}{s}$ $\frac{\lambda^1}{m}\frac{\lambda^3}{m} > \frac{0.0007}{s}$	$\frac{\lambda}{m} > \frac{0.02}{\sqrt{s}}$	$\frac{\lambda}{m} > \frac{0.02}{\sqrt{s}}$	$\frac{\lambda^1}{m} > \frac{0.02}{\sqrt{s}}$ $\frac{\lambda^2}{m} > \frac{3}{\sqrt{s}}$ $\frac{\lambda^3}{m} > \frac{58}{\sqrt{s}}$

Table 9. Best explored or explorable bilepton masses and couplings in direct high-energy searches. These are at least 95% confidence bounds. The future collider limits assume the validity of the luminosity scaling law (71)

	LEP (Z^0)	e^-e^-	e^+e^-	$e^-\gamma$
L_1^-	$m < 44$ GeV		$m < 0.5\sqrt{s}$	$m < \min\left(0.6, 12\sqrt{\sum_\ell \lambda_{e\ell}^2}\right)\sqrt{s}$
$\tilde{L}_1^{--}$	$m < 45$ GeV	$m < \sqrt{s}$		
$L_{2\mu}^-$	$m < 45$ GeV		$m < 0.5\sqrt{s}$	$m < \min\left(0.3, 26\sqrt{\sum_\ell \lambda_{e\ell}^2}\right)\sqrt{s}$
$\tilde{L}_{2\mu}^{--}$	$m < 38$ GeV	$m < \sqrt{s}$		
L_3^0	$m < 44$ GeV			
L_3^-	$m < 44$ GeV		$m < 0.5\sqrt{s}$	$m < \min\left(0.6, 12\sqrt{\sum_\ell \lambda_{e\ell}^2}\right)\sqrt{s}$
$\tilde{L}_3^{--}$	$m < 45$ GeV	$m < \sqrt{s}$		

5 Conclusion

We have derived the most general renormalizable bilepton lagrangians consistent with the $SU(2)_L \otimes U(1)_Y$ symmetry. Concentrating on those 7 bileptons which carry lepton number $L = 2$, we have provided a compilation of the present constraints from low-energy experiments, and the present and future bounds which may be set by colliders.

The model independent low-energy limits are listed in Table 3 and 4. They usually involve flavour non-diagonal couplings, so their implications are difficult to judge. We make three representative assumptions about the structure of the coupling constant matrices, and present the low-energy bounds with these assumptions in Tables 6, 5 and 7. Bileptons with masses above 100 GeV to 10 TeV, and gauge or Yukawa strength couplings would in general be consistent with the data.

Future high-energy e^+e^- and e^-e^- experiments at a linear collider of the next generation may significantly extend the present low-energy bounds, as is summarized in Table 9. Moreover, if real bileptons can be produced on-shell the observation of their decay modes will provide

unambiguous information about the structure of the coupling constant matrix. In particular, the e^-e^- linear collider mode is ideally suited for searching doubly-charged bileptons, whereas singly-charged bileptons can be well sought for in e^+e^- or $e^-\gamma$ collisions.

Acknowledgements. We are very grateful to Milan Locher for his careful reading of the entire manuscript and his numerous critical comments and suggestions. We also wish to thank David Bailey for useful conversations.

Appendix A Four-fermion vertices

Calculating bounds using 4-fermion vertices assumes that the bilepton masses are heavier than the energy scale of the experiment, so that the momentum of the bilepton in the propagator can be neglected

$$\frac{1}{p^2 - m_L^2} \to \frac{-1}{{m_L}^2} \tag{A.1}$$

The four-fermion vertices listed in the second column of Table 2 are easily derived from the lagrangian (3). They are of the form

$$\frac{a\lambda^2}{m_L^2}(\bar\psi\Gamma\chi)(\bar\epsilon\Gamma\delta)\ , \tag{A.2}$$

where ψ, χ, ϵ and δ are *chiral* fermions, the Γs are either 1 or γ^μ, and a includes all the factors of 2.

The form (A.2) may not convenient for comparing bilepton rates with standard model ones. However, by appropriate Fierz transformations and transpositions of matrix elements, the relevant bilepton four-fermion vertices can all be brought in the standard model-like $(V \pm A)(V \pm A)$ or $(V + A)(V - A)$ forms. For this operation the following relations turn out to be useful

$$(\bar a^c \gamma^\mu P_{L,R} b^c) = -(\bar b \gamma^\mu P_{R,L} a) \tag{A.3}$$

$$(\bar a P_L b)(\bar c P_R d) = -\frac{1}{2}(\bar a \gamma^\mu P_R d)(\bar c \gamma_\mu P_L b) \tag{A.4}$$

$$(\bar a \gamma^\mu P_{L,R} b)(\bar c \gamma_\mu P_{L,R} d) = (\bar a \gamma^\mu P_{L,R} d)(\bar c \gamma_\mu P_{L,R} b) \tag{A.5}$$

Note that scalar and vector bileptons do not induce any tensor matrix elements. The only way to generate matrix elements of the form $(\bar\psi\sigma^{\mu\nu}\chi)(\bar\epsilon\sigma_{\mu\nu}\delta)$ from the exchange of a scalar or vector particle is by Fierz-rearranging a scalar induced four fermion vertex where the scalar coupled to left-handed fermions at one end, and right-handed at the other (operators of the form $(\bar\psi R\chi)(\bar\epsilon R\delta)$). The standard model symmetries do not allow scalar bileptons with such interactions.

Appendix B The Cramér-Rao limit

The asymptotic resolution [85] with which a reaction can set bounds on a given parameter, say the lepton-bilepton coupling λ, is given by the Cramér-Rao limit

$$\chi^2_\infty = \mathcal{L} \int d\Omega\ \frac{\left(\frac{d\sigma(\lambda)}{d\Omega} - \frac{d\sigma(0)}{d\Omega}\right)^2}{\frac{d\sigma(0)}{d\Omega}}\ , \tag{B.1}$$

where $\sigma(0)$ is the standard model expectation and $d\Omega$ is a phase space element. The N standard deviation exclusion bounds for λ are obtained by setting $\chi^2_\infty = N^2$ in (B.1).

If the systematic errors are small, this limit is closely approached by a maximum likelihood estimator. Indeed, defining the probability density

$$p = \frac{1}{\sigma}\frac{d\sigma}{d\Omega}\ , \tag{B.2}$$

for small values of λ (B.1) can be rewritten

$$\chi^2_\infty = n\lambda^2 \int d\Omega\ \frac{1}{p}\left(\frac{\partial p}{\partial\lambda}\right)^2\Bigg|_{\lambda=0} = \lambda^2 \left\langle -\frac{\partial^2 \ln L}{\partial\lambda^2}\Bigg|_{\lambda=0}\right\rangle\ , \tag{B.3}$$

where n is the total numebr of events. Equation (B.3) defines the maximum likelihood estimator [51], where

$$L = \prod_{i=1}^{n} p(\Omega_i) \tag{B.4}$$

is the maximum likelihood function.

To prove that this is indeed the Cramér-Rao minimum variance bound, we set $\chi^2_\infty = 1$ in (B.3). Discretizing into infinitesimal phase space bins labeled i, we have $p(\Omega_i) = n_i/n$ and we obtain for the inverse dispersion of λ

$$D(\lambda)^{-1} = \frac{1}{\lambda^2}\Bigg|_{\chi^2_\infty=1} = \sum_i \frac{1}{n_i}\left(\frac{\partial n_i}{\partial\lambda}\right)^2\ . \tag{B.5}$$

By definition, n_i is the average number of events in bin i. The observed number of events N_i in this bin is distributed according to Poisson statistics, *i.e.*,

$$p_i = \frac{n_i}{n} = \frac{e^{-n_i} n_i^{N_i}}{N_i!} \tag{B.6}$$

is the probability to find N_i events in bin i. Assuming there are no bin-to-bin correlations, we have

$$< N_i > \ = \ n_i \tag{B.7}$$

$$< (N_i - n_i)(N_j - n_j) > \ = \ \delta_{ij} n_i \tag{B.8}$$

and we can rewrite (B.5)

$$D(\lambda)^{-1} = \sum_{i,j}\left\langle \left(\frac{N_i}{n_i} - 1\right)\left(\frac{N_j}{n_j} - 1\right)\right\rangle \frac{\partial n_i}{\partial\lambda}\frac{\partial n_j}{\partial\lambda}$$

$$= \left\langle \left(\sum_i \left(\frac{N_i}{n_i} - 1\right)\frac{\partial n_i}{\partial\lambda}\right)^2\right\rangle\ . \tag{B.9}$$

This is nothing but the Cramér-Rao minimum variance bound

$$D(\lambda)^{-1} = \left\langle \left(\sum_i \frac{\partial \ln p_i}{\partial \lambda} \right)^2 \right\rangle . \qquad \text{(B.10)}$$

To derive this result, we only assumed the absence of bin-to-bin correlations in (B.8). Note that no assumption concerning the population of the bins is necessary. Equation (B.1) provides thus a convenient means for computing the Cramér-Rao bound of an experiment, which in practice can be closely approached by the maximum likelihood estimator if the systematic errors are small. In the presence of real data the maximum likelihood function (B.4) can easily be evaluated with all experimental resolutions and efficiencies folded in [86].

A more detailed treatment of this issue is provided in [87].

References

1. P. Frampton, Int. J. Mod. Phys. **A11** (1996) 1621
2. W. Buchmüller, R. Rückl, D. Wyler, Phys. Lett. **B191** (1987) 442
3. S. Davidson, D. Bailey, B. Campbell, Z. Phys. **C61** (1994) 613 [hep-ph/9309310]; M. Leurer, Phys. Rev. **D49** (1994) 333 [hep-ph/9309266], ibid. **D50** (1994) 536 [hep-ph/9312341]
4. T.P. Cheng, L. Li, Phys. Rev. **D 22** (1980) 2860
5. G.B. Gelmini, M. Roncadelli, Phys. Lett. **B 99** (1981) 411
6. A. Zee, Phys.Lett. **B 93** (1980) 389
7. R. Peccei, The Physics of Neutrinos, in Proceedings of the Flavour Symposium, Peking University, August 1988
8. T. Rizzo, Phys. Rev. **D 25** (1982) 1355
9. H. Georgi, M. Machacek, Nucl. Phys. **B 262** (1985) 463; K.S. Babu, V.S. Mathur, Phys. Lett. **B 196** (1987) 218
10. For left-right models, see, for instance: J.C. Pati, A. Salam, Phys.Rev. **D10** (1974) 275; R.N. Mohapatra, J.C. pati, Phys. Rev. **D11** (1975) 566, ibid. 2558; G. Senjanovic, R.N. Mohapatra, Phys. Rev. **D 12** (1975) 1502; R.N. Mohapatra, G. Senjanovic, Phys. Rev. **D 23** (1981) 165
11. P.H. Frampton, B.H. Lee, Phys. Rev. Lett. **64** (1990) 619
12. P.B. Pal, Phys. Rev. **D 43** (1991) 236
13. P. Frampton Phys. Rev. Lett. **69** (1992) 2889; F. Pisano, V. Pleitez Phys. Rev. **D46** (1992) 410 [hep-ph/9206242]
14. P. Frampton, Mod. Phys. Lett. **A7**, (1992) 2017
15. For a review of technicolour theories, see for instance: G.G. Ross "Grand Unified Theories", (1985) Benjamin-Cummins, Menlo Park; E. Fahri, L. Susskind, Phys. Rep. **74**(1981) 277; E. Eichten et al., Rev. Mod. Phys. **56** (1984) 579. For a review of composite theories, see for instance: W. Buchmüller, Acta Phys. Austr. Suppl XXVII (1985) 517; B. Schrempp, Proc. of the XXIII Int. Conf. on High Energy Physics Berkeley
16. A.J. Davies, X. He, Phys. Rev. **D 43** (1991) 225
17. K. Mursula, M.Roos, F. Scheck, Nucl. Phys. **B 219** (1983) 321
18. K. Mursala, F. Scheck, Nucl. Phys. **B 253** (1985) 189
19. V. Barger, H.Baer, W.Y. Keung, R.J.N. Phillips, Phys.Rev. **D 26** (1982) 218
20. M.D. Swartz, Phys. Rev. **D 40** (1989) 1521
21. K. Sasaki, Phys. Lett. **B 308** (1993) 297
22. K. Ishikawa, K. Kiriyama, S. Midorikawa, T. Moriya, M. Yoshimura, Prog. Theor. Phys. **57** (1977) 1359
23. R.N. Mohapatra, J.D. Vergados, Phys. Rev. Lett. **47** (1981) 1713
24. F. Bergsma et al., Phys. Lett. **B 122** (1983) 465
25. G.K. Leontaris, K. Tamvakis, J.D. Vergados, Phys, Lett. **B 162** (1985) 153
26. J.D. Vergados, Phys. Rep. **133** (1986) 1
27. D. Chang, W. Keung, Phys. Rev. Lett. **62** (1989) 2583
28. E. Carlson, P. Frampton, Phys. Lett. **B 283** (1992) 123
29. P. Frampton, D. Ng, Phys. Rev. **D 45** (1992) 4240
30. H. Fujii, S. Nakamura, K. Sasaki, Phys. Lett. **B 299** (1993) 342
31. H. Fujii, Y. Mimura, K. Sasaki, T. Sasaki, Phys.Rev. **D49** (1994) 559 [hep-ph/9309287].
32. K. Horikawa, K. Sasaki, Phys.Rev. **D53** (1996) 560. [hep-ph/9504218]
33. A. Halprin, Phys. Rev. Lett. **48** (1982) 1313
34. W. Hollik, F. Schrempp, B. Schrempp, Phys. Lett. **140 B** (1984) 424
35. J.A. Grifols, A. Mendez, G.A. Schuler, Mod. Phys. Lett. **A 4** (1989) 1485
36. J.F. Gunion, J.A. Grifols, A. Mendez, B. Kayser, F. Olness, Phys. Rev. **D 40** (1989) 1546
37. P. Herczeg, R.N. Mohapatra, Phys. Rev. Lett. **69** (1992) 2475
38. J.A. Coarasa, A. Mendez, J. Sola, Phys.Lett. **B374** (1996) 131. [hep-ph/9511297]
39. M. Swartz, Phys. Rev. Lett. **64** (1990) 2877
40. N. Leporé et al., Phys. Rev. **D 50** (1994) 2031 [hep-ph/9403237]
41. OPAL Collaboration, Phys. Lett. **B295** (1992) 347
42. E. Accomando, S. Petrarca, Phys. Lett. **B323** (1994) 212 [hep-ph/9403237]; E. Accomando et al., Rome preprint NI-1051-11-4-95 [hep-ph/9505274]
43. P. Frampton, D. Ng, T.W. Kephart, T.C. Yuan, Phys. Lett. **B 317** (1993) 369
44. A. Pich, J.P. Silva, Phys. Rev. **D** (1995) 4006
45. J.F. Gunion, H.E. Haber, G. Kane, S. Dawson, The Higgs Hunters Guide, Addison-Wesley, (1990)
46. R. Vega, D.A. Dicus, Nucl. Phys. **B329** (1990) 533
47. K. Huitu em et al., Helsinki preprint HU-SEFT-R-1996-16 [hep-ph/9606311]
48. P. Kaus, S. Meshkov, Mod. Phys. Lett. **A3** (1988) 1251; H. Fritzsch, J. Plankl, Phys. Lett. **B237** (1990) 451
49. A. Antaramian, L.J.Hall, A. Rasin, Phys. Rev. Lett. **69** (1992) 1871
50. M. Fukugita, T. Yanagida, Phys. Rev. Lett. **58** (1987) 1807
51. The Particle Data Book, Phys.Rev. **D 50** (1994)
52. F. Scheck, Phys. Rep. **44** (1978) 187
53. A. Jodidio, Phys. Rev. **D 34** (1986) 1967; ibid. **D 37** (1986) 237
54. D.A. Krakauer et al., Phys. Lett. **B263** (1991) 534
55. U. Bellgardt et al., Nucl. Phys. **B299** (1988) 1
56. J. D. Bjorken, S. Weinberg, Phys. Rev. Lett. **38** (1977) 622
57. R.D. Bolton et al., Phys. Rev. **D38** (1988) 2077
58. A. Czarnecki, B. Krause, W.J. Marciano Phys.Rev.Lett. **76** (1996) 3267-3270

59. S.R. Moore, K. Whisnant, B. Young, Phys. Rev. **D 31** (1985) 105
60. J.P. Leveille, Nucl. Phys. **B 137** (1978) 63
61. W. Bertl, Proceedings of the Workshop Weak & Electromagnetic Interactions in Nuclei, Osaka, June 1995, Eds: H. Ejiri, T. Kishimoto, T. Sato; R.Abela et al., Phys. Rev. Lett **77** (1996) 1950
62. W.J. Marciano, A. Sirlin, Phys. Rev. **D 35** (1987) 1672
63. W. Fetscher, H. Gerber, in Precision Tests of the Standard Model, edited by P.Langacker (World Scientific, Singapore, 1993)
64. H.S. Chen, talk at XVII International Symposium on Lepton Photon Interactions, August 1995
65. K.G. Hayes et al., Phys. Rev. **D 25** (1982) 2869
66. Crystal Ball Collaboration, S. Keh et al., Phys. Lett. **B 212** (1988) 123
67. T. Bowcock et al., Phys. Rev. **D 41** (1990) 805
68. K.K. Gan, Phys. Lett. **B 209** (1988) 95
69. JADE Collaboration, Z. Phys. **C 30** (1986) 371
70. TASSO Collaboration, Z. Phys. **C 37** (1988) 171
71. E.J. Eichten, K. Lane, M. Peskin, Phys. Rev. Lett. **50** (1983) 811
72. J. Erler, Phys. Rev. **D 52** (1995) 28; F. Caravaglios, G.G. Ross, Phys. Lett. **B 346** (1995) 159
73. Y. Grossman, Phys. Lett. **B 359** (1995) 141
74. G. Drexlin et al., KARMEN collaboration, Prog. Part. Nucl. Phys **32** (1994) 375; Nucl. Phys. **B38** (1995) 235 (Proc. Suppl.)
75. N. Ushida et al., Phys. Rev. Lett. **57** (1986) 2897
76. B. Kayser, E. Fischbach, S.P. Rosen, H. Spivak, Phys. Rev. **D 20** (1979) 87
77. Allen et al., Phys. Rev. **D 47** (1993) 11
78. G.L. Fogli, Europhys. Lett. **4** (1987) 527
79. A comprehensive bibliography of high-energy e^-e^- scattering can be found at the URL `http://pss058.psi.ch/e-e-.html`
80. T. Rizzo, Phys. Rev. **D 46** (1992) 910
81. M. Lusignoli, S. Petrarca, Phys. Lett. **B226** (1989) 397
82. J.F. Gunion, Int. J. Mod. Phys. **A11** (1996) [hep-ph/9510350]
83. J.E. Spencer, Int. J. Mod. Phys. A **11** (1996) 1675
84. I.F. Ginzburg, G.L. Kotkin, V.G. Serbo, V.I. Telnov, Nucl. Instr. Meth. **205** (1983) 47
85. W.T. Eadie et al., Statistical Methods in Experimental Physics, North Holland, 1971
86. T. Barklow, SLAC-PUB-6618
87. F. Cuypers, Proceedings of the Workshop Perspectives for Electroweak Interactions in e^+e^- Collisions, Schloß Ringberg, 1995, World Scientific, Ed.: B. Kniehl [hep-ph/9503252]
88. G.W.S. Hou, Proceedings of the 3rd International Conference on $\mu^+\mu^-$ Colliders, San Francisco, 13-15 December 1995, [hep-ph/9605204]